*The Company of* **Biologists**

## RESEARCH ARTICLE

# Type-B response regulators of rice play key roles in growth, development and cytokinin signaling

Jennifer M. Worthen[1], Maria V. Yamburenko[1], Jeewoo Lim[1], Zachary L. Nimchuk[2], Joseph J. Kieber[2] and G. Eric Schaller[1,*]

## ABSTRACT

Cytokinins are plant hormones with crucial roles in growth and development. Although cytokinin signaling is well characterized in the model dicot *Arabidopsis*, we are only beginning to understand its role in monocots, such as rice (*Oryza sativa*) and other cereals of agronomic importance. Here, we used primarily a CRISPR/Cas9 gene-editing approach to characterize the roles of a key family of transcription factors, the type-B response regulators (RRs), in cytokinin signaling in rice. Results from the analysis of single *rr* mutants as well as higher-order *rr21/22/23* mutant lines revealed functional overlap as well as subfunctionalization within members of the gene family. Mutant phenotypes associated with decreased activity of rice type-B RRs included effects on leaf and root growth, inflorescence architecture, flower development and fertilization, trichome formation and cytokinin sensitivity. Development of the stigma brush involved in pollen capture was compromised in the *rr21/22/23* mutant, whereas anther development was compromised in the *rr24* mutant. Novel as well as conserved roles for type-B RRs in the growth and development of a monocot compared with dicots were identified.

KEY WORDS: *Oryza sativa*, Cytokinin, Hormone, Panicle, Crop, Yield

## INTRODUCTION

Cytokinins are phytohormones that regulate diverse aspects of plant growth and development, including cell division, shoot and root architecture, seed yield, senescence, and stress responses (Hwang et al., 2012; Kieber and Schaller, 2014; Sakakibara, 2006). Our understanding of the metabolism and perception of cytokinin has made great strides in recent years, mostly from studies of the model dicot *Arabidopsis* (Hwang et al., 2012; Kieber and Schaller, 2014). The initial pathway for cytokinin signal transduction is a multistep phosphorelay that incorporates cytokinin receptors (HKs), histidine-containing phosphotransfer proteins (AHPs) and type-B RRs. These relay the cytokinin signal from the membrane to the nucleus, where the type-B RRs function as transcription factors to regulate gene expression. The type-B RRs are structurally related, each having a receiver domain that is phosphorylated on a conserved aspartate residue, as well as a C-terminal extension with a Myb-like DNA-binding domain (Hosoda et al., 2002; Imamura et al., 1999; Raines et al., 2016; Zubo et al., 2017). Type-A *RR*s are among the targets the expression of which is induced by the type-B RRs, and these function as negative feedback regulators for the cytokinin

response (Kieber and Schaller, 2014; To et al., 2004). The type-B and type-A *RR* gene families have undergone lineage-specific expansion in monocots and dicots (Pils and Heyl, 2009; Tsai et al., 2012), suggesting that, although they have similar ancestral functions, the monocot RRs have also acquired novel functions distinct from their roles in dicots.

We know surprisingly little about the role of cytokinin in monocots, given the agronomic significance of cereals, loss-of-function studies having probably been hampered by functional overlap within the gene families. Rice is an ideal species to elucidate the role of cytokinin because of its small genome size, the availability of reference genome sequences and its ease of transformation (Devos and Gale, 2000). Indeed, genetic studies have revealed that individual genes involved in cytokinin biosynthesis and degradation can have significant roles in the development of the rice inflorescence. Disruption of *LOG*, which is involved in cytokinin biosynthesis, results in failure to maintain meristematic cells in their inflorescence meristems and, consequently, a smaller panicle and reduced grain yield (Gu et al., 2015; Kurakawa et al., 2007). By contrast, reduced expression of *CKX2*, which is involved in cytokinin degradation, results in elevated cytokinin levels and a larger panicle (Ashikari et al., 2005; Yeh et al., 2015). More recently, a mutation of the cytokinin receptor gene *HK6* was found to reduce the root sensitivity to cytokinin (Ding et al., 2017), and targeting of two *AHP*s by RNAi resulted in the production of smaller panicles along with a decrease in cytokinin sensitivity (Sun et al., 2014).

According to the model for cytokinin signaling, the type-B RRs have a pivotal role in the early transcriptional response of plants to cytokinin. Here, we used a clustered regularly interspaced short palindromic repeats (CRISPR)/Cas9 gene-editing approach to target the four most abundant type-B *RR*s of rice. Results from the analysis of single *rr* mutants as well as higher-order *rr21/22/23* mutant lines revealed functional overlap as well as subfunctionalization within members of the gene family. Mutant phenotypes associated with decreased activity of rice type-B RRs included effects on leaf and root growth, panicle architecture, flower development, trichome formation and cytokinin sensitivity. These results reveal novel as well as conserved roles for type-B RRs in the growth and development of a monocot compared with dicots. Given the gene conservation among the cereals, the roles for the type-B RRs elucidated in rice have implications for other cereal crops, such as maize and wheat.

## RESULTS

### Generation of type-B *RR* mutants by CRISPR/Cas9 gene editing

We used a CRISPR/Cas9 approach to generate loss-of-function mutations in rice type-B *RR*s. We focused on subfamily 1 members of the rice type-B *RR* family (Fig. S1A), because these have the most abundant expression and are phylogenetically related to

[1]Department of Biological Sciences, Dartmouth College, Hanover, NH 03755, USA. [2]Department of Biology, University of North Carolina, Chapel Hill, NC 27599, USA.

*Author for correspondence (george.e.schaller@dartmouth.edu)

J.J.K., 0000-0002-5766-812X; G.E.S., 0000-0003-4032-2437

DEVELOPMENT

members of the *Arabidopsis* type-B RR family implicated in cytokinin signaling (Argyros et al., 2008; Ishida et al., 2008; Tsai et al., 2012). Furthermore, *RR22* of rice complements an *Arabidopsis* subfamily 1 loss-of-function mutant, demonstrating an ability to mediate the cytokinin response *in planta* (Tsai et al., 2012). We constructed a CRISPR/Cas9 vector to edit the four most abundant rice type-B RRs of subfamily 1 (*RR21*, *RR22*, *RR23* and *RR24*) based on their expression level in shoots, roots and early panicle meristems (Figs S1 and S2). Targets for gene editing were chosen to be within 87 bp downstream of the translation start sites of the *RR*s, such that mistranslation because of frameshift mutations would occur before the receiver domain.

The CRISPR/Cas9 vector was introduced into the *Japonica* rice cultivar Kitaake by *Agrobacterium*-mediated transformation and indel mutations in *RR*s identified by sequencing. We focused on lines with frameshift mutations because these are predicted to be null mutations (Table S1). Mutations were brought to homozygosity and the CRISPR/Cas9 vector eliminated by segregation to stabilize the mutants. In this manner, we obtained the *rr21/22/23* triple mutant from three independent transformation events (E1, E2 and E4; Table S2), the characterization of which is our main focus in this study. The three independent events giving rise to the *rr21/22/23* triple mutants resulted in three different indel mutations for *rr21* and *rr22*, with each predicted to result in a frameshift and premature termination during translation (Table S2). We also obtained the single mutants *rr21*, *rr22* and *rr23*, both *rr21* and *rr23* being isolated from the same transformation event (E4) from which we also obtained an *rr21/22/23* triple mutant (Tables S1 and S2). As an additional control, we also isolated a wild-type sibling from the E4 transformation event.

### Disruption of type-B *RR*s results in altered shoot development

When grown on soil, mature plants of all three *rr21/22/23* lines (events E1, E2, and E4) exhibited phenotypes that significantly distinguished them from the wild-type controls, Wt-Kit and Wt-E4 (Fig. 1A,B). On average, plant height of the mutant decreased by 16% compared with wild type. The mutant produced more tillers compared with the wild type, although there was a decrease in the productive tillers (those that produce a panicle). The increase in tillering of the *rr21/22/23* lines arose, in part, because of the production of more secondary tillers compared with the wild type. The effect on tiller number and productive tillers was not observed in the single *rr* mutants, indicative of functional overlap in the control of this phenotype. The decrease in panicle formation by the tillers indicates a decreased ability to produce an inflorescence meristem, the increase in tiller production potentially arising as a compensatory mechanism for this defect.

The *rr21/22/23* plants were shorter than the wild type at least in part because their leaves were shorter and narrower than those of the wild type (Fig. 1C; Fig. S3A,B). The flag leaves of *rr21/22/23* averaged 77% of the length, 85% of the width and 65% of the area of the wild-type flag leaves. To determine whether the decrease in leaf size of *rr21/22/23* was because of changes in cell proliferation and/or cell expansion, we examined epidermal cells on the adaxial surface of the flag leaf (Fig. 1C). In the mutant, a decrease in cell width to 87% of the wild type accounted for the similar decrease in leaf width. By contrast, cell length was similar for the mutant and wild type (the mutant was 99.5% of the wild-type cell length on average), indicating that the decrease in leaf length was the result of a decrease in longitudinal cell proliferation.

### Disruption of type-B *RR*s results in altered panicle development

Architecture of the rice inflorescence (panicle) is derived from the meristematic structure of the reproductive meristem. The rice panicle comprises a main axis (rachis) with several primary and secondary branches, each of which produces the floral structures, called spikelets (Fig. S3C). Panicles of the *rr21/22/23* mutants were smaller and had reduced branching compared with the wild type (Fig. 1A,D). The *rr21/22/23* mutants exhibited a significant decrease in panicle length (Fig. S3D) and in the number of primary and secondary branches (Fig. 1A,D). Although the number of branches decreased, there was not a uniform effect on the primary and secondary branch lengths of the triple mutants, which were similar to those of the wild type (Fig. S3D). The effects of the *rr21/22/23* mutations on panicle architecture resulted in a significant decrease in the total number of spikelets per panicle (Fig. 1A,D). Examination of single *rr* mutants indicated that mutations in *RR21* and *RR23* contributed most significantly to the panicle phenotypes found in *rr21/22/23* (Fig. 1A,D; Fig. S3D). Overall, we observed a substantial branching defect in the *rr21/22/23* mutants, consistent with a reduced ability to produce primary and secondary branch meristems.

### Reduced fertility of the *rr21/22/23* mutant because of defective stigma development

The *rr21/22/23* mutants displayed a significant reduction in grain fill (Fig. 2A), which, combined with the ∼50% reduction in spikelet production, resulted in a drastic decrease in the grain yield per panicle for *rr21/22/23* (Fig. 2A). The grain that was produced exhibited a slight but significant decrease in grain length, but no significant difference in grain width or the 100-grain weight, and the mutant grain germinated at a rate >90% (Fig. S4A). This is suggestive of a defect in fertilization in *rr21/22/23* rather than in grain development.

To identify the basis for the decreased grain fill in the *rr21/22/23* mutants, we dissected the floral components from the spikelet just before dehiscence. Anthers from the triple mutant were developmentally normal and produced pollen with a viability >84% (Fig. S4B). However, the carpels lacked the brush structure on the stigma that aids pollen capture, hydration, and guidance of the pollen tube toward the ovary in grasses, probably accounting for the poor grain fill (Fig. 2B) (Heslop-Harrison and Reger, 1988; Heslop-Harrison et al., 1984). Examination of single *rr* mutants indicated that mutation of *RR22* contributed most to the stigma brush phenotype.

Stigma brushes are generated from a type of trichome specialized for pollen capture (Heslop-Harrison and Reger, 1988; Heslop-Harrison et al., 1984), each brush hair in rice being multicellular and branched (Fig. 2C,D). We compared stigma brush development of *rr21/22/23* to that of the wild type, establishing stages of brush development based on the phenotypic characteristics of wild type. As shown for wild type in Fig. 2C, epidermal bulges appear early during stigma development (stage 1), give rise to multicellular brush primordia (stage 2), begin and complete the formation of multicellular branches (stages 3 and 4) and undergo cell expansion (stage 5) to form the branched multicellular hairs that comprise the stigma brush. Each hair, including its branches, is several cells thick as well as multiple cells in length, consistent with growth involving both periclinal and anticlinal cell divisions. By contrast, in the *rr21/22/23* mutant, brush hairs were delayed in initiation, more randomly distributed along the stigma and deficient in periclinal and anticlinal divisions, such that they prematurely aborted growth (Fig. 2C,D).
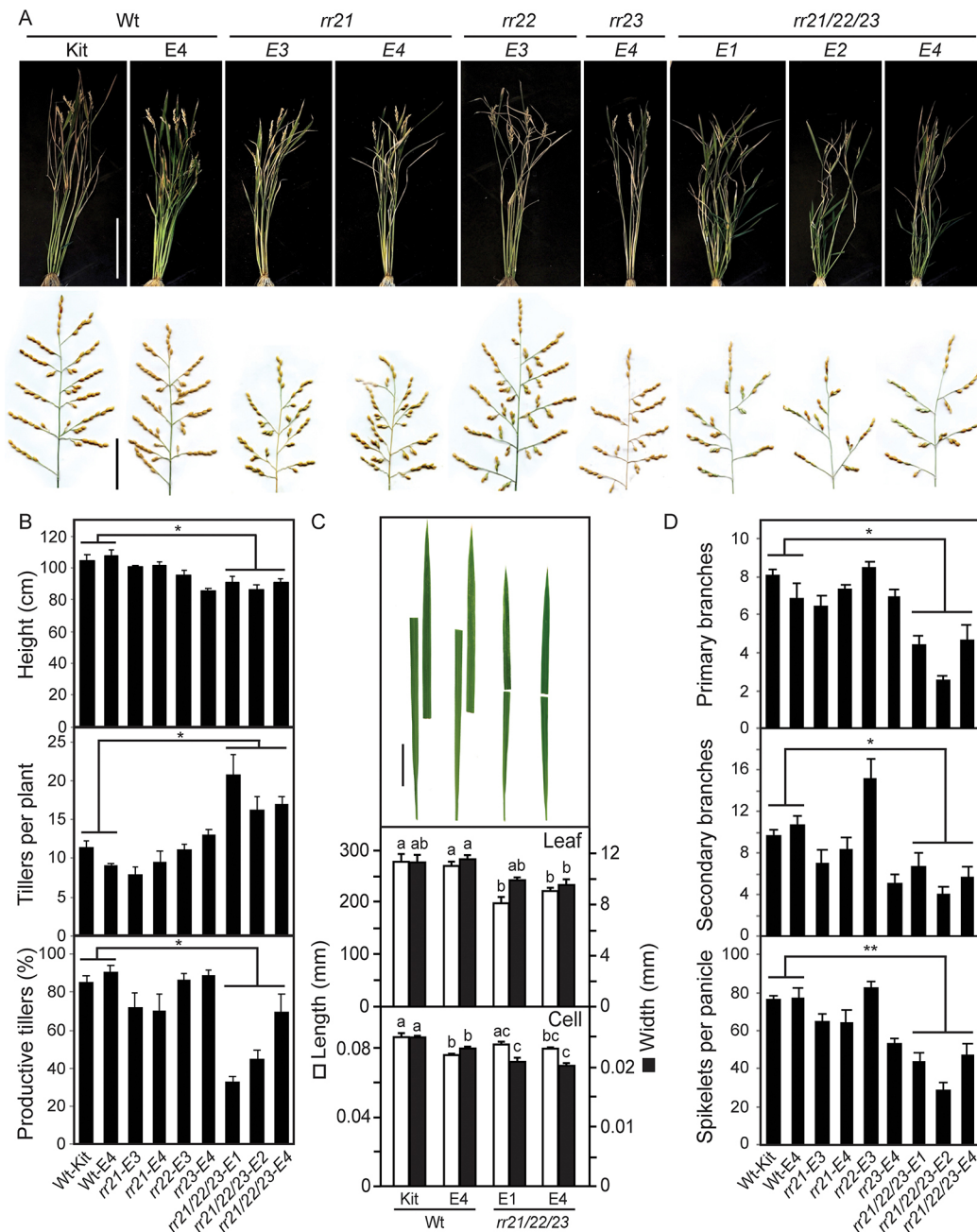
**Fig. 1. Shoot and panicle phenotypes of type-B *rr* mutants.** (A) Shoots and panicles of mature *rr* mutant plants. (B) Plant height, number of tillers per plant and percentage of productive tillers per plant (*n*≥6). (C) Flag leaf characteristics showing leaf images, leaf length and width (*n*=5), and cell length and width (*n*=70). Different letters indicate significant differences at *P*<0.05. (D) Panicle architecture parameters, including numbers of primary branches, secondary branches and spikelets per panicle (*n*≥8). For data comparison of *rr21/22/23* lines with wild type (B,D), ANOVA was performed with post hoc Holm multiple comparison calculation. *ial*P*<0.05, **ar*P*<0.01; error bars show s.e.m. Scale bars: 30 cm (shoots in A); 6 cm (panicles in A; leaves in C).

However, the brush cells produced in the mutant were still capable of expansion to a similar degree to that observed in the wild type (Fig. 2C,D). Although cell proliferation associated with growth of the stigma brush hairs was severely impacted by the *rr21/22/23* mutant, the rest of the carpel appeared to grow normally (Fig. 2B,C) and was still capable of being fertilized, indicative that the defect in cell proliferation was localized to the brush itself.

To gain insight into the underlying molecular differences between the stigmas in wild type and *rr21/22/23*, we examined the expression of selected genes previously identified as enriched for expression in the rice stigma (Li et al., 2007). For this purpose, carpels with

stage 5 brushes were used based on the developmental stage analyzed by Li et al. (2007). We examined the expression of the transcription factors *GL3A*, a rice homolog of *GLABRA3* of *Arabidopsis*, the homeobox-Leu zipper protein *HOX2*, and *NPR5/BOP*, which regulates rice leaf and flower development (Toriba et al., 2019). Expression of both *GL3A* and *HOX2* was significantly reduced in *rr21/22/23* compared with wild type (Fig. 2E), expression of *GL3A* being particularly compromised in the mutant and potentially correlating with the presence of multiple type-B RR DNA-binding motifs in its regulatory regions [one six-mer DNA-binding motif is found at the promoter/5′-untranslated region (UTR) junction, two in
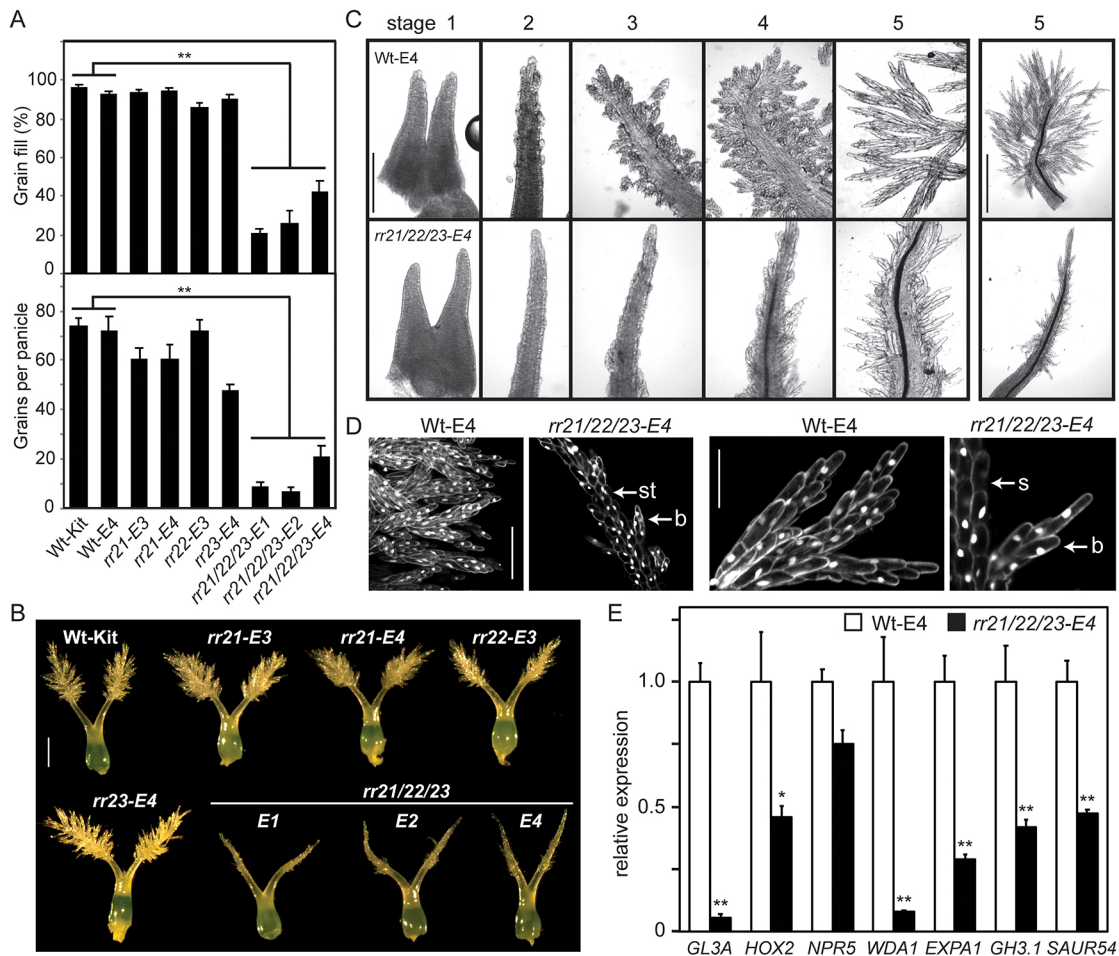
**Fig. 2. Effect of type-B *rr* mutants on stigma brush development.** (A) Reduced grain fill and grains per panicle in *rr21/22/23* mutants. For data comparison of *rr21/22/23* lines to wild type, ANOVA was performed with post hoc Holm multiple comparison calculation (**$P<0.01$; $n\geq8$; error bars show s.e.m.). (B) Malformed brush structure on stigma of *rr21/22/23* mutants. (C) Characteristics of stigma development in Wt-E4 and *rr21/22/23-E4*. (D) Fluorescence imaging of DAPI-stained brush hairs (stage 5) to reveal nuclei and cell boundaries. For Wt-E4, just the branched multicellular brush hairs are shown. For *rr21/22/23-E4*, the prematurely aborted brush hairs (b) are shown protruding from the stigma tip (st) and stigma (s). (E) Expression analysis by RT-qPCR of genes normally enriched for expression in wild-type stigma ($n=4$; *$P<0.05$, **$P<0.01$, *t*-test; error bars show s.e.m.). Genes chosen for analysis were from Li et al. (2007). Scale bars: 0.5 mm [B and stage 5 (right) in C]; 0.2 mm [stages 1-5 (left) in C]; 50 µm (D, right); 100 µm (D, left).

the 5′-UTR region and three in the first large intron of the coding region] (Raines et al., 2016). Expression of two cell wall-related genes (*WDA1* and *EXPA6*) was also reduced in the mutant (Fig. 2E), *WDA1* being a *CER*-like gene involved in cuticle wax biosynthesis (Jung et al., 2006). Genes related to auxin responses are enriched for expression in the rice stigma (Li et al., 2007), and so we also examined the expression of SAUR54 and the indole-3-acetic acid (IAA)-amido synthetase *GH3.1*, expression of both of which was significantly reduced in *rr21/22/23* compared with wild type (Fig. 2E). Although not reported to be enriched in the stigma, we also examined *WOX3B* and *HL6* because these genes are implicated in the regulation of rice leaf trichome formation (Sun et al., 2017), but found their expression too variable in the carpels to allow for accurate assessment. Taken together, these data demonstrate substantial changes in gene expression related to the defective stigma brush development in *rr21/22/23*, the effects on *GL3A* and *WDA1* being the most pronounced of the genes examined.

### Disruption of type-B *RR*s results in altered trichome development

Given that stigma brushes are generated from a specialized type of trichome, defects in their production can coincide with the inability

to produce other types of trichome (Heslop-Harrison and Reger, 1988; Heslop-Harrison et al., 1984; Li et al., 2010). Therefore, we examined *rr21/22/23* for additional defects in trichome development, uncovering a substantial decrease in trichome initiation and elongation on the grain hulls, with the single *rr22* mutant again contributing most to this phenotype (Fig. 3A,B). The trichomes on the hulls are substantially different from those on the stigma, being single celled and unbranched compared with multicellular and branched. Leaves of *rr21/22/23* still produced macrotrichomes, although these differed in two respects from the wild type; first, they were largely absent from the abaxial leaf surface and, second, where present on the adaxial surface and leaf margin, they were smaller than those of the wild type (Fig. 3C).

### Mutants of *RR24* are infertile because of defective anther development

Similar to *rr21/22/23*, *rr24* mutants also exhibited a drastic reduction in grain fill. We identified two independent mutants lacking a functional *RR24*, one from a T-DNA insertion population (*rr24*) and the second as a result of our CRISPR/Cas9 mutational analysis (an *rr23/24* double mutant). Both lines were completely infertile and were maintained in the hemizygous state for *rr24*. We performed a
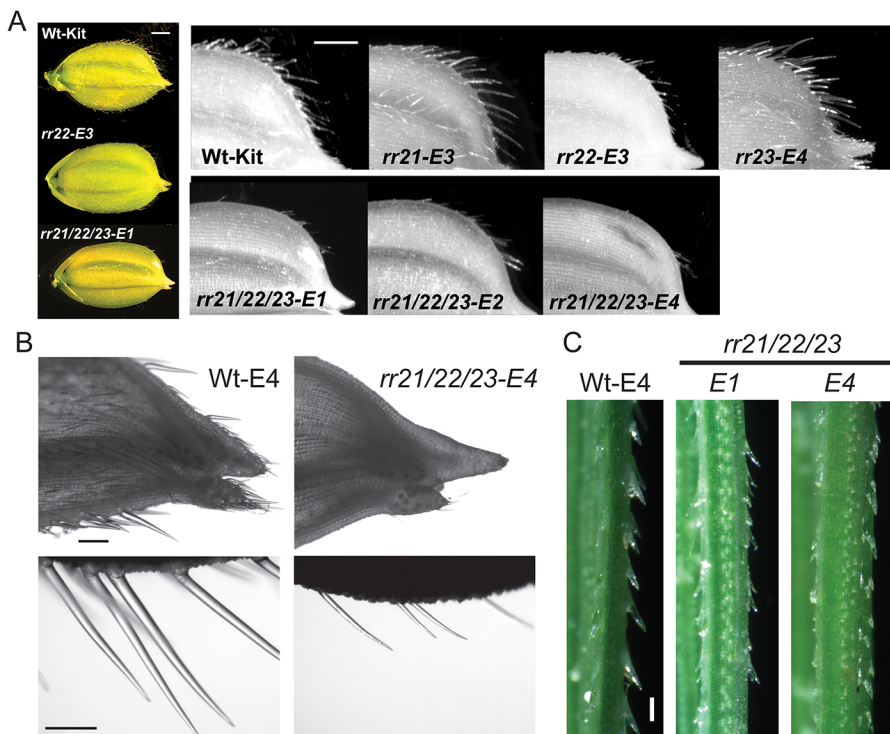
**Fig. 3. Effect of type-B *rr* mutants on trichome development.** (A) Reduced trichome production on hulls of *rr21/22/23* mutants, showing complete hulls (left) and close-up images (right). (B) Close-up images of trichomes on hulls of Wt-E4 and *rr21/22/23-E4*. (C) The *rr21/22/23* lines developed smaller macrotrichomes compared with wild type. Macrotrichomes along the margin of the mature flag leaf are shown. Scale bars: 1 mm (A); 0.2 mm (B); 0.1 mm (C).

detailed characterization of the *rr24* T-DNA insertion line (Fig. S5A,B). Panicles of the *rr24* mutant were not significantly different from those of their wild-type siblings based on panicle length, primary and secondary branch numbers, primary branch length, spikelets per panicle and panicles per plant (Fig. 4A,B). We also did not observe any obvious differences in *rr24* compared with wild type in terms of shoot growth, leaf size or mass of the root system. Nevertheless, unlike either the wild type or the $RR24^{+/-}$

hemizygote, spikelets of the homozygous *rr24* mutant exhibited no grain fill, resulting in no seed being produced from the panicle (Fig. 4C). Dissection of the floral components from the spikelet just before dehiscence revealed that *rr24* had a normal carpel and stigma brush, but a severely malformed anther with no detectable pollen. This phenotype was confirmed by examination of the floral components of the *rr23/24* CRISPR/Cas9-induced mutant (Fig. S5C). The specificity of the *rr24* mutant phenotype is
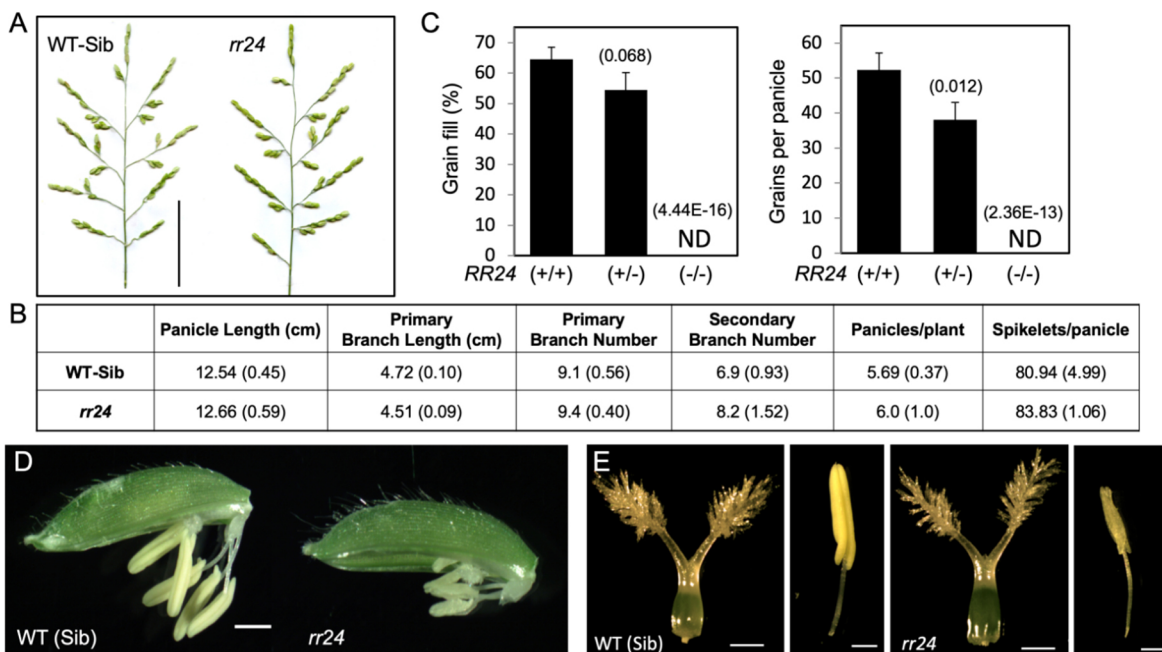


**Fig. 4. *rr24* mutants produce infertile panicles with a wild type-like architecture.** (A) Panicles of *rr24* T-DNA mutant and its wild-type sibling. (B) Panicle architecture parameters for *rr24* mutant compared with wild-type sibling. Parameters were not significantly different (*t*-test *P*<0.05; *n*=10); s.e. in parentheses. (C) Grain fill per panicle (%) and total grain per panicle for $RR24^{+/+}$, $RR24^{+/-}$ and $RR24^{-/-}$ ($n\geq13$). *P*-values are indicated for comparison to the wild type ($RR24^{+/+}$) based on ANOVA performed with post-hoc Holm comparison calculation. (D) Dissected spikelets of *rr24* and its wild-type sibling. (E) Stigmas and anthers of *rr24* and its wild-type sibling. Scale bars: 6 cm (A); 1 mm (D); 0.5 mm (E). ND, not detected.

| | Panicle Length (cm) | Primary Branch Length (cm) | Primary Branch Number | Secondary Branch Number | Panicles/plant | Spikelets/panicle |
|---|---|---|---|---|---|---|
| WT-Sib | 12.54 (0.45) | 4.72 (0.10) | 9.1 (0.56) | 6.9 (0.93) | 5.69 (0.37) | 80.94 (4.99) |
| rr24 | 12.66 (0.59) | 4.51 (0.09) | 9.4 (0.40) | 8.2 (1.52) | 6.0 (1.0) | 83.83 (1.06) |

consistent with analyses indicating that the expression of *RR24* increases when floral meristems are produced and that *RR24* is the most highly expressed type-B *RR* in mature anthers (Li et al., 2007; Patel et al., 2012; Yamburenko et al., 2017).

## Effects of type-B *RR* mutants on root development

Rice has a fibrous root system, similar to maize and other monocots, and this comprises a seminal root, crown roots and both small and large lateral roots (Rebouillat et al., 2009). The crown roots are similar to adventitious roots in that they emerge from stem nodes. This fibrous root system differs from the taproot system of *Arabidopsis*, which is mostly derived from the embryonic primary root. In 10-day-old rice seedlings grown on Kimura's media solidified with agar, we observed a decrease in both shoot and root growth for *rr21/22/23* compared with wild type (Fig. 5A,B). The decrease in shoot growth (Wt-Kit=10.1 cm; Wt-E4=9.4 cm; *rr21/22/23*-E1=7.0 cm; *rr21/22/23*-E4=7.2 cm; triple mutants significantly different from wild type, *P*<0.01) was consistent with effects of the mutations on the growth of mature, soil-grown plants (Fig. 1A-C). Characterization of root growth parameters for *rr21/22/23* indicated that it had shorter seminal roots, along with a decrease in lateral root formation compared with wild type (Fig. 5A,B). The reduction in root growth was unexpected based on the model established in *Arabidopsis* and tobacco, in which cytokinin is generally considered an inhibitor of root growth and loss of type-B RRs can result in increased primary root growth (Dello Ioio et al., 2007; Hill et al., 2013; Werner et al., 2003; Werner et al., 2010). Given that we observed differences in rice growth dependent on the media, we confirmed a similar root phenotype for *rr21/22/23* seedlings grown in hydroponic culture with Yoshida's media (Fig. 5C) (Yoshida et al., 1976). The seminal root meristem of *rr21/22/23* was smaller than that in wild type, indicating that the reduction in root growth of the mutant was the result, at least in part, of a decrease in cell proliferation (Fig. 5D).

## Altered cytokinin response in the *rr21/22/23* mutant

The major role established for type-B RRs is in mediating cytokinin signal transduction; therefore, we assessed the cytokinin sensitivity of the *rr21/22/23* mutants. For this purpose, we used a

dark-induced leaf senescence assay and a root-growth response assay, and also examined gene expression in response to exogenous cytokinin. For the dark-induced leaf senescence assay, wild-type leaves lost their chlorophyll after 5 days in the dark, but this effect could be reversed by the inclusion of cytokinin in the media (Fig. 6A). The initial chlorophyll levels in the flag leaves of *rr21/22/23* were similar to those of wild type, but the mutant was less sensitive to cytokinin for reversing the dark-induced senescence, indicating that type-B RRs are required for this cytokinin-mediated response.

For the rice seminal root, as with the *Arabidopsis* primary root, exogenous cytokinin inhibits elongation. Therefore, we compared the effect of cytokinin on growth of the wild-type and *rr21/22/23* seminal roots. Treatment with cytokinin inhibited growth of the seminal root in wild-type seedlings (Fig. 6B,C). By contrast, although the seminal roots of *rr21/22/23* were shorter than those of wild type (Fig. 5), their growth was not significantly inhibited by exogenous cytokinin (Fig. 6B,C). Thus, based on physiological assays for both the shoot and root, *rr21/22/23* was less sensitive to cytokinin compared with the wild type, consistent with the positive role of type-B *RR*s in mediating the cytokinin response.

The type-B RRs are transcription factors and, thus, we also examined cytokinin-dependent gene expression in the *rr21/22/23* lines. For this purpose, we examined the expression of *RR6*, *RR9/10* and *CKX5*, which are likely to be cytokinin primary-response genes directly regulated by the type-B RRs based on their rapid induction, induction in both shoots and roots and extended DNA motifs in their promoters for type-B RR binding (Raines et al., 2016). Cytokinin-dependent expression was examined at 1 and 4 h in roots and shoots following cytokinin treatment, because primary-response genes often exhibit an initial increase followed by a decrease in their expression in response to signal. The induction of these genes by cytokinin was significantly reduced in the *rr21/22/23* lines compared with the wild type (Fig. 7). Thus, as with the physiological assays, the molecular assays indicated that the shoots and roots of *rr21/22/23* are less sensitive to cytokinin compared with the wild type, consistent with the positive role of type-B *RR*s in regulating cytokinin-responsive gene expression.
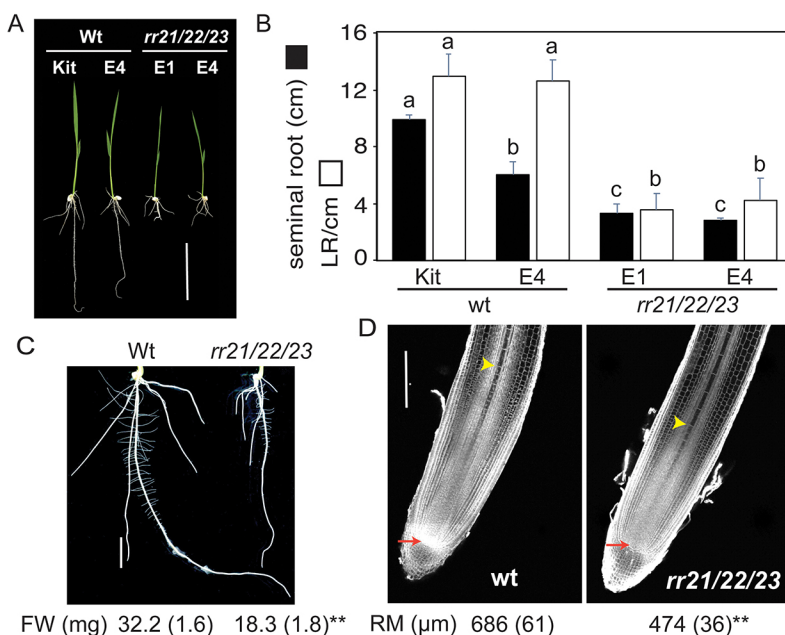


**Fig. 5. Root phenotypes of type-B *rr* mutants.** (A) Ten-day-old seedling phenotypes of Wt (Kitaake and Wt sibling of CRISPR event 4) and *rr21/22/23* (two independent CRISPR events, E1 and E4) grown in Kimura's media. (B) Seminal root length and lateral roots/cm on the seminal root for Wt and *rr21/22/23* lines. ANOVA was performed with post hoc Holm multiple comparison calculation. Different letters indicate significant differences at *P*<0.01 (*n*≥9). (C) Reduced root growth of *rr21/22/23*-E4 compared with Wt-E4 when grown hydroponically in Yoshida's media for 7 days (*n*≥9; **P*<0.01 *t*-test). (D) Root meristem length of *rr21/22/23*-E4 compared with Wt-E4 (*n*≥5; **P*<0.01 *t*-test); s.e. in parentheses. Red arrows indicate quiescent centers and yellow arrowheads indicate the upper end of root meristem based on the central metaxylem cell file. Scale bars: 5 cm (A); 1 cm (C); 200 µm (D). FW, mean fresh weight of roots; RM, root meristem.
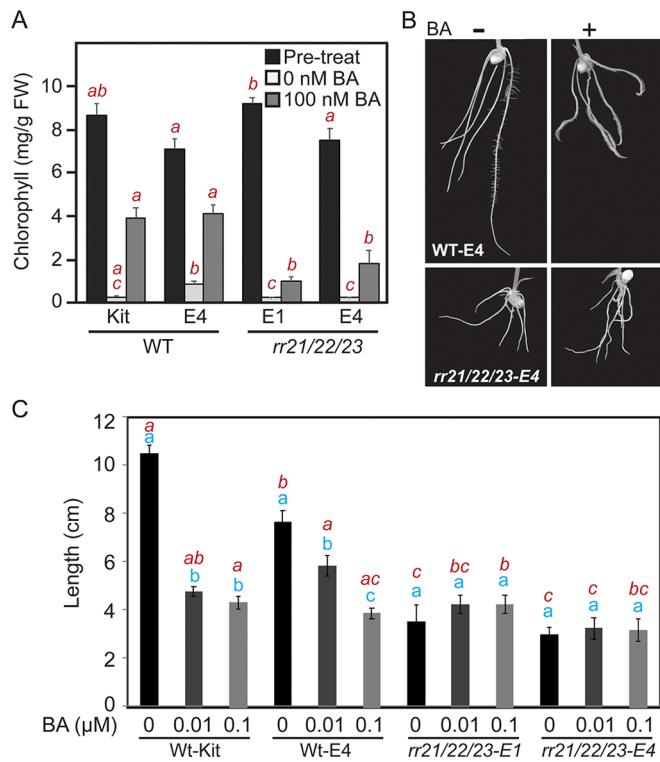
**Fig. 6. Reduced cytokinin sensitivity of *rr21/22/23* mutant based on dark-induced leaf senescence and root growth response.** (A) Effect of exogenous cytokinin (BA) on dark-induced leaf senescence (*n*=10). Flag leaf segments were incubated in the dark for 5 days in the absence or presence of 100 nM BA and then analyzed for chlorophyll retention. Chlorophyll was also isolated from leaf segments before the assay (Pre-treat) for comparison. (B) Root growth of Wt and *rr21/22/23* in the presence and absence of cytokinin (0.1 µM BA). (C) Quantification of seminal root-growth response to cytokinin (*n*≥8). ANOVA was performed with post hoc Holm multiple comparison calculations (B and C); blue lettering indicates a statistical comparison within a genotype for the cytokinin response; red lettering indicates a statistical comparison at the same cytokinin concentration across genotypes. Different letters indicate significant differences at *P*<0.05.

## DISCUSSION

Relatively little is known in monocots regarding cytokinin signaling in general, and almost nothing is known regarding the roles of type-B RRs in particular. Here, we took advantage of a CRISPR/Cas9 gene-editing approach to functionally characterize the roles of the four most abundant type-B *RR*s in rice growth and development. This approach uncovered novel roles for type-B *RR*s in a monocot, along with evidence for functional overlap and subfunctionalization within the gene family (summarized in Fig. S6). Functional overlap was revealed by additive effects for mutations in *RR21*, *RR22* and *RR23* on tillering, leaf growth, panicle architecture, grain fill, stigma brush and trichome formation. Subfunctionalization was indicated based on greater relative contributions of individual family members to various developmental characteristics. For example, *RR21* and *RR23* contributed more to leaf growth than *RR22*, whereas *RR22* contributed the most to stigma brush and trichome formation, and *RR24* mutants exhibited a specific defect in anther development. The roles uncovered for type-B RRs in rice growth and development are likely to arise primarily because they also mediate the transcriptional response to cytokinin, based on the decreased sensitivity of the shoot and root to cytokinin observed in the *rr21/22/23* mutants and the relevance to various cytokinin-related responses, as described below.

Our results are consistent with a positive role for rice type-B *RR*s in meristem activity and cell proliferation in the shoot. A role in meristem activity is indicated by the decreased ability of *rr* mutant tillers to form panicles and, when formed, by defects in their architecture. Panicle architecture is determined by meristems that give rise to the branches and spikelets, and mutants affecting cytokinin biosynthesis and degradation have revealed a crucial role for cytokinin in regulating this phenotype (Ashikari et al., 2005; Gu et al., 2015; Kurakawa et al., 2007; Yeh et al., 2015). *RR21* and *RR23* are expressed early during panicle meristem development, consistent with the defects in primary and secondary branch formation arising from their loss (Yamburenko et al., 2017). A role for type-B *RR*s in cell proliferation was indicated by the decrease in leaf size and cell number in the *rr21/22/23* mutant. Similarly, a type-B *RR* triple mutant of *Arabidopsis* also exhibits smaller leaves with fewer cells (Argyros et al., 2008). In rice, given the structured cell organization of the leaf, a specific defect in longitudinal but not in latitudinal cell proliferation was uncovered in the *rr* mutant.

Type-B *RR* mutants affected various aspects of flower development. Analysis of the rice *log* mutant indicates a greater role for cytokinin in rice flower development than is found in *Arabidopsis*. The *log* mutant of rice fails to develop floral organs, and was so named because it sometimes produces a single stamen and no pistil (Kurakawa et al., 2007); by contrast, the *ahk* triple cytokinin-receptor mutant of *Arabidopsis* produces relatively normal-looking flowers (Kinoshita-Tsujimura and Kakimoto, 2011). The floral whorls were still produced in the rice type-B *RR* mutants, allowing us to discriminate specific roles for the family members in pistil and stamen development. A defect in stigma brush formation was uncovered in *rr21/22/23*, with *rr22* contributing most to this phenotype. The stigma brush of grasses aids in pollen capture, hydration and guidance of the pollen tube toward the ovary, its loss likely accounting for the poor grain fill observed in *rr21/22/23* (Heslop-Harrison and Reger, 1988; Heslop-Harrison et al., 1984).

The stigma brush of grasses is considered a trichome-like structure because it is derived from epidermal cells and its development is sensitive to mutations that disrupt leaf trichome formation (Heslop-Harrison and Reger, 1988; Heslop-Harrison et al., 1984). Nevertheless, the structure of the stigma brush of grasses can be considerably more complex than that we generally associate with trichomes, even that of multicellular glandular trichomes. The hairs on the rice brush are not only multicellular, but also branched, each hair being several layers of cells thick and ~0.5 mm in length. We identified stages of cell proliferation, branching and elongation in the development of the rice stigma brush, the *rr21/22/23* mutant being particularly compromised in cell proliferation and branching. In *rr21/22/23*, the substantial decrease in expression for *WDA1*, a *CER*-like gene involved in cuticle wax biosynthesis (Jung et al., 2006), probably relates to the decrease in overall surface area for the stigma brush in the mutant. Of potentially greater interest is our finding that expression of *GL3A*, a rice homolog of *GLABRA3* of *Arabidopsis*, was decreased in *rr21/22/23*. In *Arabidopsis*, the transcription factor GL3 has a key role in leaf trichome formation; however, it is unclear how well the *Arabidopsis* model translates to other plant species (Liu et al., 2016; Zheng et al., 2016).

A defect in anther development was uncovered in *rr24* mutants; RR24 is a rice type-B RR that exhibits maximal expression during later stages of panicle meristem development when floral organs are produced and also maintains a high level of expression in the anther itself (Li et al., 2007; Patel et al., 2012; Yamburenko et al., 2017).
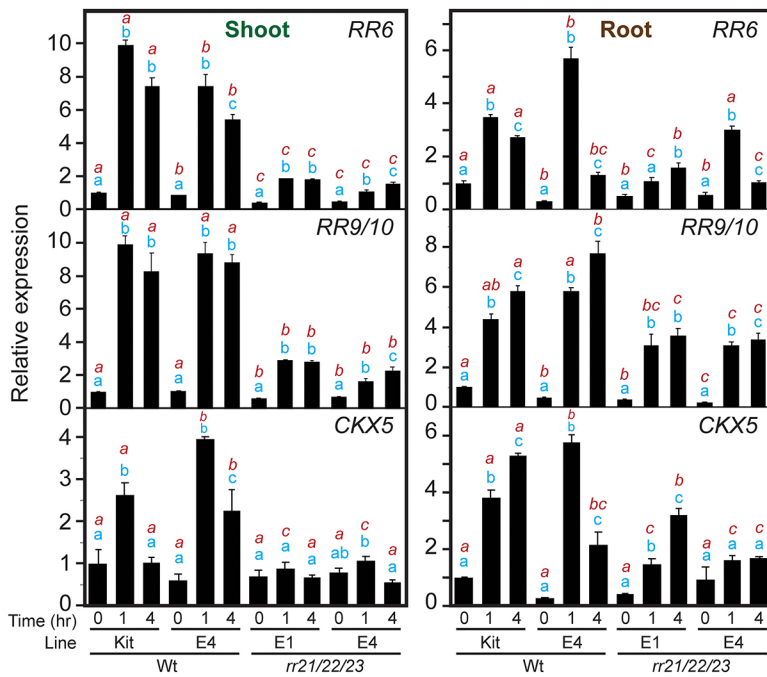
**Fig. 7. Shoots and roots of *rr21/22/23* mutants exhibit a reduced response to cytokinin based on gene expression analysis by RT-qPCR.** Seven-day-old seedlings were treated with 5 µM BA for the indicated times and gene expression in shoots and roots analyzed by RT-qPCR. ANOVA was performed with a post-hoc Holm multiple comparison calculation; blue lettering indicates a statistical comparison within a genotype for the cytokinin response; red lettering indicates a statistical comparison at the same cytokinin concentration across genotypes. Different letters indicate significant differences at *P*<0.05 (*n*=3).

An *RR24* mutation was also recently uncovered independently in a forward genetic screen to identify the basis for sterility in the rice *lepto1* mutant (Zhao et al., 2018), the pollen mother cells in this mutant arresting early during prophase I of meiosis, thereby accounting for the lack of pollen production. Previously, expression of a *CKX* gene in maize resulted in male-sterile plants lacking viable pollen (Huang et al., 2003), consistent with *RR24* mediating a cytokinin-dependent developmental process.

Type-B *RRs* regulate trichome development based on the mutant analysis. Treatment with exogenous cytokinin was previously found to stimulate trichome initiation in *Arabidopsis* and rice (Maes and Goossens, 2010; Maes et al., 2008), although the *ahk* triple cytokinin-receptor mutant of *Arabidopsis* still produces trichomes (Nishimura et al., 2004), raising questions as to the significance of the exogenous cytokinin studies. Analysis of the rice type-B *rr* mutants suggested roles in different stages of trichome development. They affected not only the initiation of trichome development from epidermal cells based on the decreases observed in leaf trichome number, but also subsequent development based on decreases in trichome size, this being most noticeable in the stigma brush hairs, which failed to elongate.

Based on the model established in *Arabidopsis*, cytokinin primarily serves as a negative regulator of root growth (Dello Ioio et al., 2007; Hill et al., 2013; Werner et al., 2003; Werner et al., 2010)]. However, analysis of the rice *rr21/22/23* mutant supported both negative and positive roles for type-B RRs in regulating root growth. A negative role for cytokinin in rice root growth was supported by the inhibitory effects of exogenous cytokinin; *rr21/22/23* exhibited reduced responsiveness to exogenous cytokinin treatment, consistent with type-B RRs mediating this response. A positive role for cytokinin in rice root growth was supported based on the *rr21/22/23* mutant exhibiting shorter seminal roots, along with a decrease in lateral root formation, compared with wild type. This growth defect is similar to what might be predicted if the *rr21/22/23* lines were hypersensitive to cytokinin, but that interpretation is not consistent with their decreased cytokinin sensitivity based on root physiological and molecular response assays. Similar to *rr21/22/23*, *AHP-RNAi* lines and an *HK6* mutant

of rice exhibit reduced root growth sensitivity to exogenous cytokinin treatment (Ding et al., 2017; Sun et al., 2014), but did not have the smaller initial root system found in *rr21/22/23*. However, *rr21/22/23* was more compromised than these other rice mutants for two-component signaling, based on its panicle and seed set defects; therefore, novel developmental phenotypes might be uncovered in its analysis. The decrease in root meristem size in the *rr21/22/23* mutant suggests that type-B RRs and, by extension, cytokinin signaling, can have a positive role in cell proliferation. A model consistent with these observations is that a low level of type-B RR activity is needed to maintain cell proliferation at the root meristem, whereas higher levels of type-B RR activity are inhibitory. Such a model might also apply to dicots but has not yet been adequately tested because higher-order mutants in the *Arabidopsis* cytokinin signaling pathway result in aborted primary root growth, possibly because cell divisions needed to establish the vasculature during its initial embryonic patterning are missing (Argyros et al., 2008; De Rybel et al., 2014; Hutchison et al., 2006; Nishimura et al., 2004).

## MATERIALS AND METHODS
### Plant materials and growth conditions
CRISPR/Cas9 mutants were developed in *Oryza sativa* ssp. *Japonica* cv. Kitaaki. The T-DNA insertion line for *RR24* (Line ID: M0003103) was obtained from the TRIM mutant population in the *Japonica* rice cultivar Tainung 67 (Hsing et al., 2007); *rr24* contains the T-DNA insert in the second exon, as confirmed by sequencing, and was maintained as a hemizygote for the insertion because of infertility of the homozygote. For plants grown in soil, a 1:1 ratio of Pro-mix BX Mycorrhizae and Profile Porous Ceramic Greens Grade was used, supplemented with water-soluble nitrogen/phosphorous/potassium (NPK) fertilizer (20-20-20; 2.9 g/l) and iron (Fe) fertilizer (Sprint 330; 0.48 g/l). Plants were grown in a greenhouse at 30°C during the day and 25°C at night, using a 10-h light/14-h dark cycle as described elsewhere (Yamburenko et al., 2017). For growth of seedlings on media, dehusked seed was sterilized with 50% (v/v) bleach solution for 30 min, washed with sterile water, germinated at 37°C for 16 h and then generally transferred to one-half strength Kimura's medium (Yoshida et al., 1976) solidified with 0.4% (w/v) Phytoagar (PlantMedia) and grown at 30°C/28°C with a 12-h light/12-h dark cycle (light=400 µE).

## CRISPR/Cas9 mutagenesis of *RR21*, *RR22*, *RR23* and *RR24*

A binary vector for rice transformation (pARS3_MUbCAS9_MC) was constructed for use with CRISPR/Cas9 mutagenesis (Figs S1 and S2). The backbone of the vector has a kanamycin-resistance gene (*Npt*) for bacteria selection. The T-DNA portion of the vector incorporates a transformation booster sequence (TBS) and a plant-codon-optimized hemagglutinin (HA)-tagged nuclear-localized Cas9 gene (Cas9-HA-N7), driven by the *Zea mays UBQ10* promoter and containing a ribosomal-binding site (RBS). The T-DNA also bears MCS for cloning of single guide RNAs (sgRNAs), and hygromycin resistance gene (*Hpt*) driven by the rice UBQ2 promoter for selection of transformed rice callus. A Gateway compatible version of the vector was also generated (pARS3_MUbCAS9_GW) by amplifying the Gateway cassette from the vector pEarlyGate103 using primers 5′-CTC-GAGATCAACAAGTTTGTACAAAAAAGCTGAACG-3′ and 5′-ACTA-GTTCAAGCGTAATCTGGAACATCGTATGGG-3′ and then blunt-end cloning the product into the SmaI site of pARS3_MUbCAS9_MC. Novel vector sequences have been deposited with Addgene with ID numbers 76923 and 76931.

To target *RR21*, *RR22*, *RR23* and *RR24*, a tandem CRISPR cassette was synthesized that encoded four sgRNAs driven by rice U3 promoters and surrounded by attL1 and attL2 Gateway recombination sites, and cloned into the EcoRV site of pUC57 (General Biosystems). The protospacer regions chosen for targeting were determined by use of the CRISPR-PLANT online tool developed at the Arizona Genomics Institute (Xie et al., 2014) and were designed to introduce indel mutations within 87 bp from the translation start sites of the *RR*s. The CRISPR array was recombined into the pARS3_MUbCAS9_GW vector to generate the vector CRISPR-RR21,22,23,24 (Figs S1C and S2). Transformation of Kitaake rice with CRISPR-RR21,22,23,24 in the EHA105 strain of *Agrobacterium* was performed by the Plant Transformation Facility at Iowa State University (www.biotech.iastate.edu/ptf/).

For the identification and genotyping of CRISPR/Cas9 mutants, genomic DNA was extracted from the leaves of mature plants using the cetyl trimethylammonium bromide (CTAB) extraction method (Clarke, 2009), the region surrounding the CRISPR target sequence was then amplified by PCR with gene-specific primers (Table S3) and sequenced. Indel mutations were determined by manually examining the sequencing chromatograms. The presence of the T-DNA insert with the *Cas9* cassette was determined by PCR using primers for *Hpt* (Table S3). Stable mutant lines were achieved by segregating away the T-DNA insert. If additional mutations were desired, lines hemizygous for the T-DNA insert were carried forwarded to the next generation. All lines used for physiological analysis lacked the T-DNA insert and had the mutated *RR* sequence reconfirmed by sequencing. Characteristics of the indel mutations and the lines used for study are given in Tables S1 and S2.

## Quantification of shoot, panicle, grain and root-related parameters

Quantification of physiological parameters was performed using ImageJ2 within the Fiji image-processing platform (Rueden et al., 2017; Schindelin et al., 2012), after scanning of leaves, panicles, grain or roots using an Epson Perfection V500 Photo scanner. For leaves, fully expanded flag leaves of flowering tillers from mature plants were characterized. For panicles, the largest panicle from mature plants was removed and taped to paper to spread its branches before scanning. Grain was removed from panicles and dehusked for analysis of weight, width and length. Seedlings for root analysis were grown in sterile Magenta GA-7 vessels (Carolina Biological), coupled to a second vessel to increase the height, containing 300 ml of media at a low agar concentration of 0.3% (w/v) to facilitate the removal of roots without damage. For reporting of percent differences between the *rr21/22/23* mutants and wild type, the averages were taken for the *rr21/22/23* mutant events compared with the average of the Wt-Kit and Wt-E4 controls.

## Characterization of leaf epidermal cells

Leaf epidermal cells were characterized using a modification of the method of Yoshikawa et al. (2013). The central portions of flag leaves from the flowering tillers of mature plants were fixed in formaldehyde:glacial acetic acid:50% ethanol (2:1:17) for 16 h at 4°C, followed by dehydration in a graded ethanol series. The dehydrated leaf blades were then incubated at 96°C in 8:3:1 chloral hydrate:water:glycerol (w/v/v) diluted 1:1 with 100% ethanol for 10 min followed by 22°C for 3 h. Epidermal cells near the midrib were imaged by digital image correlation (DIC) with a Nikon Eclipse 90i light microscope.

## Characterization of stigma brush development

Stigmas in wild type were assigned to five stages for brush development based on morphological characteristics (Fig. 2C). These stages were then correlated with spikelet morphology and carpel size, because these were similar in wild type and the *rr21/22/23* mutant, to allow for isolation of mutant stigma at similar stages of development. For confocal microscopy, spikelets were fixed with 1.5% (v/v) formaldehyde and 0.5% (v/v) glutaraldehyde in PEMT buffer [50 mM PIPES (1,4-piperazinediethanesulfonic acid), 2 mM EGTA, 2 mM MgSO$_4$, 0.05% (v/v) Triton X-100, pH 7.2] for 1 h under vacuum, washed three times with PEMT buffer, and then three times with cold PBS, using the buffers as described previously (Ishida et al., 2009). Stigma brushes were dissected and stained with 4′,6-diamidino-2-phenylindole (DAPI; 1 µg/ml) in PBS on microscope slides for 15 min before imaging by confocal microscopy using a 40× oil objective. Excitation was at 405 nm and emission light collected using a 450/50 nm filter.

## Characterization of root meristems

Seedlings were grown for 7 days on water-saturated paper, and the radicle root tips (0.5-1 cm) were dissected and fixed in cold FAA [50% (v/v) ethanol, 5% (v/v) glacial acetic acid, and 3.7% (v/v) formaldehyde] for 16 h at 4°C and then transferred to 70% (v/v) ethanol for storage at 4°C. Roots were dehydrated with a graded ethanol series of 80%, 90% and 100% (v/v) ethanol by incubating for 30 min in each of the solutions and then mounting on slides in methyl salicylate (wintergreen oil) for clearing. The coverslips were sealed with nail polish, and the specimens incubated on the slides with methyl salicylate for 16 h at 22°C before imaging. Autofluorescence emitted from cell walls was captured using a Nikon A1 confocal microscope with 20× oil objective. Lasers of 405 nm and 488 nm were used for excitation, and emission light collected above 482/35-nm and 540/30-nm filters, respectively. Signals from both channels were combined, and NIS-elements confocal software was used to stitch together four frames for each root image. Measurements were made using ImageJ software. Meristem length was based on the length of the central metaxylem (cmx) cell file, starting from the quiescent center and ending at the lower border of where the cmx cells begin to rapidly elongate.

## Pollen viability assay

Pollen viability was assessed by staining with iodine potassium iodide as described previously (Chhun et al., 2007). Viable pollen grains were identified by their staining black or dark brown, whereas sterile or dead pollen grains were identified by their staining orange or light red.

## Chlorophyll retention assay

Two-cm-long sections of the flag leaf, excised 2 cm up from the base of the leaf, were incubated in water with the indicated concentrations of benzyladenine (BA) for 5 days in the dark at 30°C. At the end of the incubation period, chlorophyll was extracted with 100% ethanol at 4°C for 1 day on a platform shaker. For comparison, chlorophyll was also isolated from flag leaf sections before incubation. The content of chlorophyll a+b was measured spectrophotometrically (OD$_{648}$ and OD$_{664}$) with a Spark Tecan plate reader in 96-well plates, and the amount of chlorophyll a+b per fresh weight was calculated (Ritchie, 2006).

## Gene expression analysis

Seedlings used for RT-quantitative (q)PCR analysis were grown on sterile filter paper soaked with one-half-strength Kimura liquid media in Petri dishes at 30°C/28°C with a 12-h light/12-h dark cycle (light=100 µE). Seven-day-old seedlings were then submerged in one-half-strength Kimura medium containing 5 µM BA or a NaOH vehicle control in 50-ml conical tubes for 0, 1 or 4 h. The roots and shoots were then excised and flash frozen in liquid nitrogen. Carpels used for RT-qPCR analysis were dissected from spikelets with stage-5 stigmas and collected in RNA*later* (Invitrogen), with ~30 carpels per biological replicate, before freezing in liquid

nitrogen. Frozen tissue was ground with a tissue homogenizer (Mixer Mill 400, Retsch), and total RNA extracted using the E.Z.N.A Plant RNA Kit (Omega Bio-Tek) as described previously (Yamburenko et al., 2017). DNase treatment was performed with the DNA-free DNA removal kit (Ambion), first-strand cDNA synthesis with Superscript III cDNA Synthesis Kit (Invitrogen) using poly-T primers, and RT-qPCR with the iTaq Universal SYBR Green Supermix (Bio-Rad) according to the manufacturer's instructions. RT-qPCR reactions were performed with three or four biological replicates, along with technical replicates, on the CFX384 Real-Time system (Bio-Rad). Primers used for RT-qPCR are given in Table S3. Expression of the *UBQ5* gene was used for normalization. Relative gene expression was calculated by the $\Delta\Delta$Ct method (Schefe et al., 2006).

## Microscopy
Images of epidermal cells in flag leaves were acquired using DIC with a Nikon Eclipse 90i and a Hamamatsu C11440 digital camera. For reproductive tissues, flowers were dissected and visualized using a Leica MZ16 microscope with Spot Idea software for capturing images. For fluorescence imaging of stigma brushes and root meristems, a Nikon A1 confocal microscope was used.

## Statistical analysis
Statistical analysis was performed using an online calculator (astatsa.com/OneWay_Anova_with_TukeyHSD/).

## Accession codes
Sequence data from this article can be found in the Rice Genome Annotation Project GenBank/EMBL data libraries under the following accession numbers (TIGR Locus ID): *RR21* (LOC_Os03g12350), *RR22* (LOC_Os06g08440), *RR23* (LOC_Os02g55320), *RR24* (LOC_Os02g08500), *RR6* (LOC_Os04g57720), *RR9/10* (LOC_Os11g04720), *CKX5* (LOC_Os01g56810), *GL3a* (LOC_Os04g47080), *HOX2* (LOC_Os06g04870), *NPR5/BOP1* (LOC_Os01g72020), *EXPA6* (LOC_Os03g21820), *WDA1* (LOC_Os10g33250), *GH3.1* (LOC_Os01g57610), *SAUR54* (LOC_Os09g37490), *HL6* (LOC_Os06g44750), *WOX3B* (LOC_Os05g02730) and *UBQ5* (LOC_Os03g13170).

## References
**Argyros, R. D., Mathews, D. E., Chiang, Y.-H., Palmer, C. M., Thibault, D. M., Etheridge, N., Argyros, D. A., Mason, M. G., Kieber, J. J. and Schaller, G. E.** (2008). Type B response regulators of Arabidopsis play key roles in cytokinin signaling and plant development. *Plant Cell* **20**, 2102-2116. doi:10.1105/tpc.108.059584

**Ashikari, M., Sakakibara, H., Lin, S., Yamamoto, T., Takashi, T., Nishimura, A., Angeles, E. R., Qian, Q., Kitano, H. and Matsuoka, M.** (2005). Cytokinin oxidase regulates rice grain production. *Science* **309**, 741-745. doi:10.1126/science.1113373

**Chhun, T., Aya, K., Asano, K., Yamamoto, E., Morinaka, Y., Watanabe, M., Kitano, H., Ashikari, M., Matsuoka, M. and Ueguchi-Tanaka, M.** (2007). Gibberellin regulates pollen viability and pollen tube growth in rice. *Plant Cell* **19**, 3876-3888. doi:10.1105/tpc.107.054759

**Clarke, J. D.** (2009). Cetyltrimethyl ammonium bromide (CTAB) DNA miniprep for plant DNA isolation. *Cold Spring Harb. Protoc.* **2009**, pdb prot5177. doi:10.1101/pdb.prot5177

**De Rybel, B., Adibi, M., Breda, A. S., Wendrich, J. R., Smit, M. E., Novak, O., Yamaguchi, N., Yoshida, S., Van Isterdael, G., Palovaara, J. et al.** (2014). Plant development. Integration of growth and patterning during vascular tissue formation in Arabidopsis. *Science* **345**, 1255215. doi:10.1126/science.1255215

**Dello Ioio, R., Linhares, F. S., Scacchi, E., Casamitjana-Martinez, E., Heidstra, R., Costantino, P. and Sabatini, S.** (2007). Cytokinins determine Arabidopsis root-meristem size by controlling cell differentiation. *Curr. Biol.* **17**, 678-682. doi:10.1016/j.cub.2007.02.047

**Devos, K. M. and Gale, M. D.** (2000). Genome relationships: the grass model in current research. *Plant Cell* **12**, 637-646. doi:10.1105/tpc.12.5.637

**Ding, W., Tong, H., Zheng, W., Ye, J., Pan, Z., Zhang, B. and Zhu, S.** (2017). Isolation, characterization and transcriptome analysis of a cytokinin receptor mutant Osckt1 in rice. *Front. Plant Sci.* **8**, 88. doi:10.3389/fpls.2017.00088

**Gu, B., Zhou, T., Luo, J., Liu, H., Wang, Y., Shangguan, Y., Zhu, J., Li, Y., Sang, T., Wang, Z. et al.** (2015). An-2 encodes a cytokinin synthesis enzyme that regulates awn length and grain production in rice. *Mol. Plant* **8**, 1635-1650. doi:10.1016/j.molp.2015.08.001

**Heslop-Harrison, Y. and Reger, B. J.** (1988). Tissue organisation, pollen receptivity and pollen tube guidance in normal and mutant stigmas of the grass *Pennisetum typhoides* (Burm.) Stapf et Hubb. *Sex. Plant Reprod.* **1**, 182-193. doi:10.1007/BF00193749

**Heslop-Harrison, Y., Reger, B. J. and Heslop-Harrison, J.** (1984). The pollen-stigma interaction in the grasses. 5. Tissue organization and cytochemistry of the stigma ("silk") of *Zea mays* L. *Acta Bot Neerl* **33**, 81-99. doi:10.1111/j.1438-8677.1984.tb01774.x

**Hill, K., Mathews, D. E., Kim, H. J., Street, I. H., Wildes, S. L., Chiang, Y.-H., Mason, M. G., Alonso, J. M., Ecker, J. R., Kieber, J. J. et al.** (2013). Functional characterization of type-B response regulators in the Arabidopsis cytokinin response. *Plant Physiol.* **162**, 212-224. doi:10.1104/pp.112.208736

**Hosoda, K., Imamura, A., Katoh, E., Hatta, T., Tachiki, M., Yamada, H., Mizuno, T. and Yamazaki, T.** (2002). Molecular structure of the GARP family of plant Myb-related DNA binding motifs of the Arabidopsis response regulators. *Plant Cell* **14**, 2015-2029. doi:10.1105/tpc.002733

**Hsing, Y.-I., Chern, C.-G., Fan, M.-J., Lu, P.-C., Chen, K.-T., Lo, S.-F., Sun, P.-K., Ho, S.-L., Lee, K.-W., Wang, Y.-C. et al.** (2007). A rice gene activation/knockout mutant resource for high throughput functional genomics. *Plant Mol. Biol.* **63**, 351-364. doi:10.1007/s11103-006-9093-z

**Huang, S., Cerny, R. E., Qi, Y., Bhat, D., Aydt, C. M., Hanson, D. D., Malloy, K. P. and Ness, L. A.** (2003). Transgenic studies on the involvement of cytokinin and gibberellin in male development. *Plant Physiol.* **131**, 1270-1282. doi:10.1104/pp.102.018598

**Hutchison, C. E., Li, J., Argueso, C., Gonzalez, M., Lee, E., Lewis, M. W., Maxwell, B. B., Perdue, T. D., Schaller, G. E., Alonso, J. M. et al.** (2006). The Arabidopsis histidine phosphotransfer proteins are redundant positive regulators of cytokinin signaling. *Plant Cell* **18**, 3073-3087. doi:10.1105/tpc.106.045674

**Hwang, I., Sheen, J. and Müller, B.** (2012). Cytokinin signaling networks. *Annu. Rev. Plant Biol.* **63**, 353-380. doi:10.1146/annurev-arplant-042811-105503

**Imamura, A., Hanaki, N., Nakamura, A., Suzuki, T., Taniguchi, M., Kiba, T., Ueguchi, C., Sugiyama, T. and Mizuno, T.** (1999). Compilation and characterization of *Arabidopsis thaliana* response regulators implicated in His-Asp phosphorelay signal transduction. *Plant Cell Physiol.* **40**, 733-742. doi:10.1093/oxfordjournals.pcp.a029600

**Ishida, K., Yamashino, T., Yokoyama, A. and Mizuno, T.** (2008). Three type-B response regulators, ARR1, ARR10, and ARR12, play essential but redundant roles in cytokinin signal transduction throughout the life cycle of *Arabidopsis thaliana*. *Plant Cell Physiol.* **49**, 47-57. doi:10.1093/pcp/pcm165

**Ishida, T., Fujiwara, S., Miura, K., Stacey, N., Yoshimura, M., Schneider, K., Adachi, S., Minamisawa, K., Umeda, M. and Sugimoto, K.** (2009). SUMO E3 ligase HIGH PLOIDY2 regulates endocycle onset and meristem maintenance in Arabidopsis. *Plant Cell* **21**, 2284-2297. doi:10.1105/tpc.109.068072

**Jung, K.-H., Han, M.-J., Lee, D.-Y., Lee, Y.-S., Schreiber, L., Franke, R., Faust, A., Yephremov, A., Saedler, H., Kim, Y.-W. et al.** (2006). Wax-deficient anther1 is involved in cuticle and wax production in rice anther walls and is required for pollen development. *Plant Cell* **18**, 3015-3032. doi:10.1105/tpc.106.042044

**Kieber, J. J. and Schaller, G. E.** (2014). Cytokinins. *The Arabidopsis Book* **12**, e0168. doi:10.1199/tab.0168

**Kinoshita-Tsujimura, K. and Kakimoto, T.** (2011). Cytokinin receptors in sporophytes are essential for male and female functions in Arabidopsis thaliana. *Plant Signal. Behav.* **6**, 66-71. doi:10.4161/psb.6.1.13999

Kurakawa, T., Ueda, N., Maekawa, M., Kobayashi, K., Kojima, M., Nagato, Y., Sakakibara, H. and Kyozuka, J. (2007). Direct control of shoot meristem activity by a cytokinin-activating enzyme. *Nature* **445**, 652-655. doi:10.1038/nature05504

Li, M., Xu, W., Yang, W., Kong, Z. and Xue, Y. (2007). Genome-wide gene expression profiling reveals conserved and novel molecular functions of the stigma in rice. *Plant Physiol.* **144**, 1797-1812. doi:10.1104/pp.107.101600

Li, W. Q., Wu, J. G., Wen, S. L., Zhang, D. P., Zhang, Y. J. and Si, C. H. (2010). Characterization and fine mapping of the glabrous leaf and hull mutants (gl1) in rice (*Oryza sativa* L.). *Plant Cell Rep.* **29**, 617-627. doi:10.1007/s00299-010-0848-2

Liu, X., Bartholomew, E., Cai, Y. and Ren, H. (2016). Trichome-related mutants provide a new perspective on multicellular trichome initiation and development in cucumber (Cucumis sativus L). *Front. Plant Sci.* **7**, 1187. doi:10.3389/fpls.2016.01187

Maes, L. and Goossens, A. (2010). Hormone-mediated promotion of trichome initiation in plants is conserved but utilizes species- and trichome-specific regulatory mechanisms. *Plant Signal. Behav.* **5**, 205-207. doi:10.4161/psb.5.2.11214

Maes, L., Inze, D. and Goossens, A. (2008). Functional specialization of the TRANSPARENT TESTA GLABRA1 network allows differential hormonal control of laminal and marginal trichome initiation in Arabidopsis rosette leaves. *Plant Physiol.* **148**, 1453-1464. doi:10.1104/pp.108.125385

Nishimura, C., Ohashi, Y., Sato, S., Kato, T., Tabata, S. and Ueguchi, C. (2004). Histidine kinase homologs that act as cytokinin receptors possess overlapping functions in the regulation of shoot and root growth in Arabidopsis. *Plant Cell* **16**, 1365-1377. doi:10.1105/tpc.021477

Patel, R. V., Nahal, H. K., Breit, R. and Provart, N. J. (2012). BAR expressolog identification: expression profile similarity ranking of homologous genes in plant species. *Plant J.* **71**, 1038-1050. doi:10.1111/j.1365-313X.2012.05055.x

Pils, B. and Heyl, A. (2009). Unraveling the evolution of cytokinin signaling. *Plant Physiol.* **151**, 782-791. doi:10.1104/pp.109.139188

Raines, T., Blakley, I. C., Tsai, Y.-C., Worthen, J. M., Franco-Zorrilla, J. M., Solano, R., Schaller, G. E., Loraine, A. E. and Kieber, J. J. (2016). Characterization of the cytokinin-responsive transcriptome in rice. *BMC Plant Biol.* **16**, 260. doi:10.1186/s12870-016-0932-z

Rebouillat, J., Dievart, A., Verdeil, J. L., Escoute, J., Giese, G., Breitler, J. C., Gantet, P., Espeout, S., Guiderdoni, E. and Périn, C. (2009). Molecular genetics of rice root development. *Rice* **2**, 15-34. doi:10.1007/s12284-008-9016-5

Ritchie, R. J. (2006). Consistent sets of spectrophotometric chlorophyll equations for acetone, methanol and ethanol solvents. *Photosynth. Res.* **89**, 27-41. doi:10.1007/s11120-006-9065-9

Rueden, C. T., Schindelin, J., Hiner, M. C., DeZonia, B. E., Walter, A. E., Arena, E. T. and Eliceiri, K. W. (2017). ImageJ2: ImageJ for the next generation of scientific image data. *BMC Bioinformatics* **18**, 529. doi:10.1186/s12859-017-1934-z

Sakakibara, H. (2006). Cytokinins: activity, biosynthesis, and translocation. *Annu. Rev. Plant Biol.* **57**, 431-449. doi:10.1146/annurev.arplant.57.032905.105231

Schefe, J. H., Lehmann, K. E., Buschmann, I. R., Unger, T. and Funke-Kaiser, H. (2006). Quantitative real-time RT-PCR data analysis: current concepts and the novel "gene expression's CT difference" formula. *J. Mol. Med. (Berl.)* **84**, 901-910. doi:10.1007/s00109-006-0097-6

Schindelin, J., Arganda-Carreras, I., Frise, E., Kaynig, V., Longair, M., Pietzsch, T., Preibisch, S., Rueden, C., Saalfeld, S., Schmid, B. et al. (2012). Fiji: an open-source platform for biological-image analysis. *Nat. Methods* **9**, 676-682. doi:10.1038/nmeth.2019

Sun, L., Zhang, Q., Wu, J., Zhang, L., Jiao, X., Zhang, S., Zhang, Z., Sun, D., Lu, T. and Sun, Y. (2014). Two rice authentic histidine phosphotransfer proteins, OsAHP1 and OsAHP2, mediate cytokinin signaling and stress responses in rice. *Plant Physiol.* **165**, 335-345. doi:10.1104/pp.113.232629

Sun, W., Gao, D., Xiong, Y., Tang, X., Xiao, X., Wang, C. and Yu, S. (2017). Hairy leaf 6, an AP2/ERF transcription factor, interacts with OsWOX3B and regulates trichome formation in rice. *Mol. Plant* **10**, 1417-1433. doi:10.1016/j.molp.2017.09.015

To, J. P. C., Haberer, G., Ferreira, F. J., Deruere, J., Mason, M. G., Schaller, G. E., Alonso, J. M., Ecker, J. R. and Kieber, J. J. (2004). Type-A Arabidopsis response regulators are partially redundant negative regulators of cytokinin signaling. *Plant Cell* **16**, 658-671. doi:10.1105/tpc.018978

Toriba, T., Tokunaga, H., Shiga, T., Nie, F., Naramoto, S., Honda, E., Tanaka, K., Taji, T., Itoh, J.-I. and Kyozuka, J. (2019). BLADE-ON-PETIOLE genes temporally and developmentally regulate the sheath to blade ratio of rice leaves. *Nat. Commun.* **10**, 619. doi:10.1038/s41467-019-08479-5

Tsai, Y.-C., Weir, N. R., Hill, K., Zhang, W., Kim, H. J., Shiu, S.-H., Schaller, G. E. and Kieber, J. J. (2012). Characterization of genes involved in cytokinin signaling and metabolism from rice. *Plant Physiol.* **158**, 1666-1684. doi:10.1104/pp.111.192765

Werner, T., Motyka, V., Laucou, V., Smets, R., Van Onckelen, H. and Schmülling, T. (2003). Cytokinin-deficient transgenic Arabidopsis plants show multiple developmental alterations indicating opposite functions of cytokinins in the regulation of shoot and root meristem activity. *Plant Cell* **15**, 2532-2550. doi:10.1105/tpc.014928

Werner, T., Nehnevajova, E., Köllmer, I., Novák, O., Strnad, M., Krämer, U. and Schmülling, T. (2010). Root-specific reduction of cytokinin causes enhanced root growth, drought tolerance, and leaf mineral enrichment in Arabidopsis and tobacco. *Plant Cell* **22**, 3905-3920. doi:10.1105/tpc.109.072694

Xie, K., Zhang, J. and Yang, Y. (2014). Genome-wide prediction of highly specific guide RNA spacers for CRISPR-Cas9-mediated genome editing in model plants and major crops. *Mol. Plant* **7**, 923-926. doi:10.1093/mp/ssu009

Yamburenko, M. V., Kieber, J. J. and Schaller, G. E. (2017). Dynamic patterns of expression for genes regulating cytokinin metabolism and signaling during rice inflorescence development. *PLoS ONE* **12**, e0176060. doi:10.1371/journal.pone.0176060

Yeh, S.-Y., Chen, H.-W., Ng, C.-Y., Lin, C.-Y., Tseng, T.-H., Li, W.-H. and Ku, M.-S. (2015). Down-regulation of cytokinin oxidase 2 expression increases tiller number and improves rice yield. *Rice* **8**, 36. doi:10.1186/s12284-015-0070-5

Yoshida, S., Forno, D. A., Cock, J. H. and Gomez, K. A. (1976). *Laboratory Manual for Physiological Studies of Rice*, 3rd edn. Los Banos, Laguna, Philippines: The International Rice Research Institute.

Yoshikawa, T., Eiguchi, M., Hibara, K.-I., Ito, J.-I. and Nagato, Y. (2013). Rice slender leaf 1 gene encodes cellulose synthase-like D4 and is specifically expressed in M-phase cells to regulate cell proliferation. *J. Exp. Bot.* **64**, 2049-2061. doi:10.1093/jxb/ert060

Zhao, T., Ren, L., Chen, X., Yu, H., Liu, C., Shen, Y., Shi, W., Tang, D., Du, G., Li, Y. et al. (2018). The OsRR24/LEPTO1 type-B response regulator is essential for the organization of leptotene chromosomes in rice meiosis. *Plant Cell* **30**, 3024-3037. doi:10.1105/tpc.18.00479

Zheng, K., Tian, H., Hu, Q., Guo, H., Yang, L., Cai, L., Wang, X., Liu, B. and Wang, S. (2016). Ectopic expression of R3 MYB transcription factor gene OsTCL1 in Arabidopsis, but not rice, affects trichome and root hair formation. *Sci. Rep.* **6**, 19254. doi:10.1038/srep19254

Zubo, Y. O., Blakley, I. C., Yamburenko, M. V., Worthen, J. M., Street, I. H., Franco-Zorrilla, J. M., Zhang, W., Hill, K., Raines, T., Solano, R. et al. (2017). Cytokinin induces genome-wide binding of the type-B response regulator ARR10 to regulate growth and development in Arabidopsis. *Proc. Natl. Acad. Sci. USA* **114**, E5995-E6004. doi:10.1073/pnas.1620749114
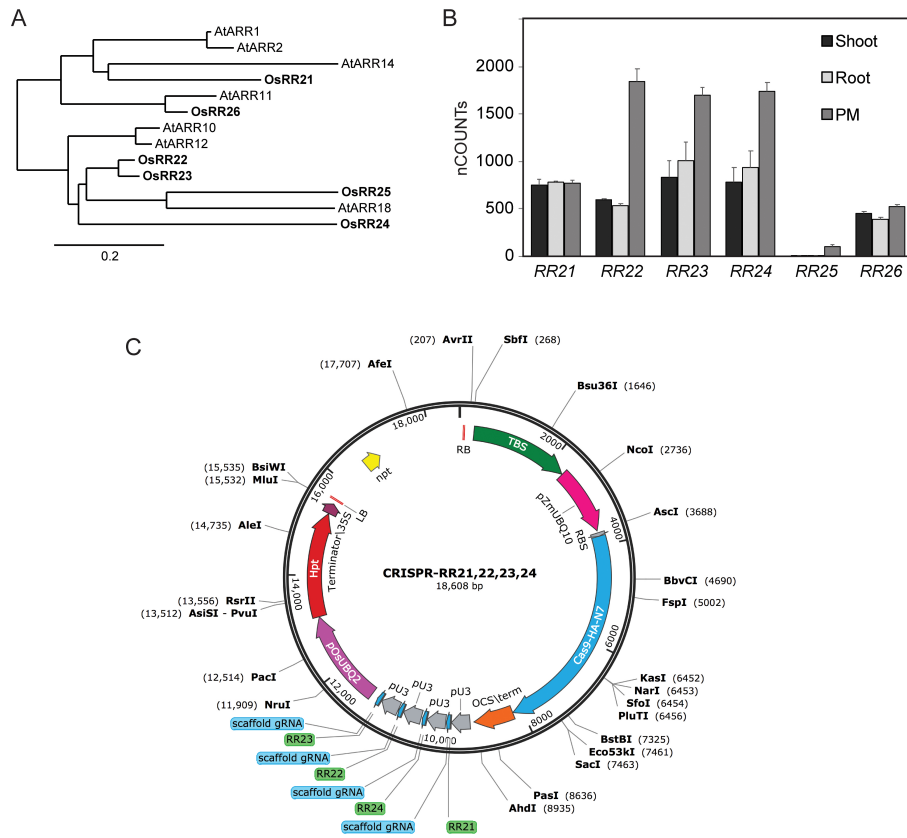
**Fig. S1.** Targeting of rice type-B RRs by a CRISPR/Cas9 approach. **A,** Subfamily-1 of the type-B RRs from rice and Arabidopsis. A phylogeny based on the receiver domains was constructed using the default parameters of the phylogeny.fr pipeline (Dereeper et al., 2008), with alignment performed using MUSCLE 3.8.31 and refined with Gblocks 0.91b, phylogeny using maximum likelihood with PhyML 3.1/3.0 (aLRT), and tree rendering with TreeDyn 198.3. Sequences from rice are in bold and designated with the prefix Os; sequences from Arabidopsis are designated with the prefix At. The nomenclature for rice and Arabidopsis RRs is as described (Schaller et al., 2008; Tsai et al., 2012). "A complete phylogenetic tree for the response regulators of rice and Arabidopsis can be found in Tsai et al. (2012)." **B,** Expression of rice type-B RRs based on Nanostring analysis. The average gene expression value is given in normalized nCounts for roots, shoots, and early panicle meristems (PM) based on published data (Tsai et al., 2012; Yamburenko et al., 2017). Error bars represent SE. **C,** Diagram of CRISPR/Cas9 construct used for targeting *RR21*, *RR22*, *RR23*, and *RR24* of rice. The T-DNA portion of the vector incorporates a transformation booster sequence (TBS) and a plant-codon-optimized HA-tagged nuclear-localized Cas9 gene (Cas9-HA-N7), driven by the *Z. mays UBQ10* promoter and containing a ribosomal binding site (RBS). The vector also incorporates a kanamycin resistance gene (Npt) for bacterial selection on its backbone, and a hygromycin resistance gene (Hpt) driven by the rice *UPQ2* promoter for selection in rice on the T-DNA. The four sgRNAs driven by rice *U3* promoters to target *RR21*, *RR22*, *RR23*, and *RR24* were introduced into a Gateway site by recombination.
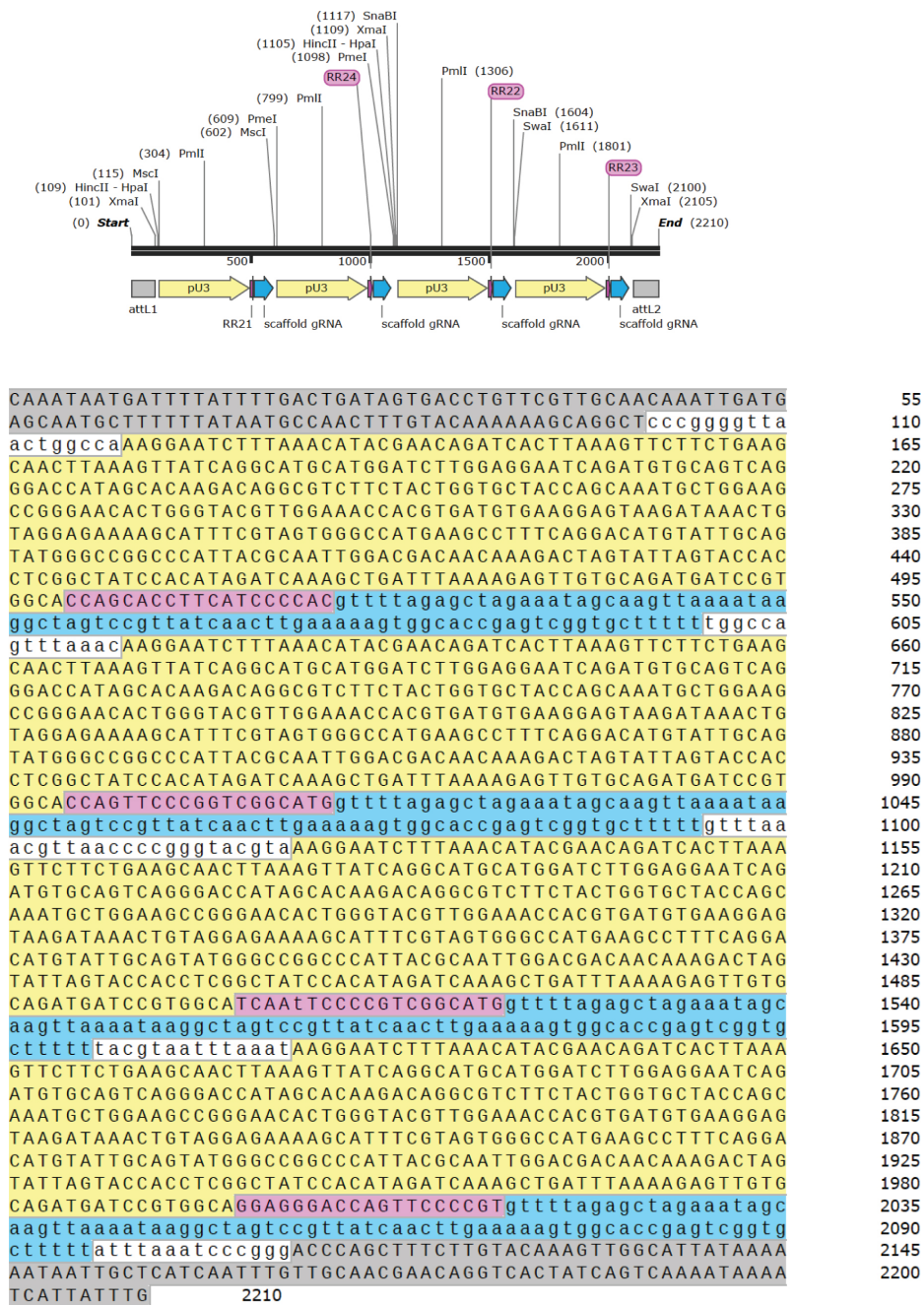
**Fig. S2.** Map and sequence for the CRISPR insert targeting *RR21*, *RR22*, *RR23*, and *RR24*. The same colors used to indicate portions of the insert in the map (top) are used to highlight the sequence (bottom).
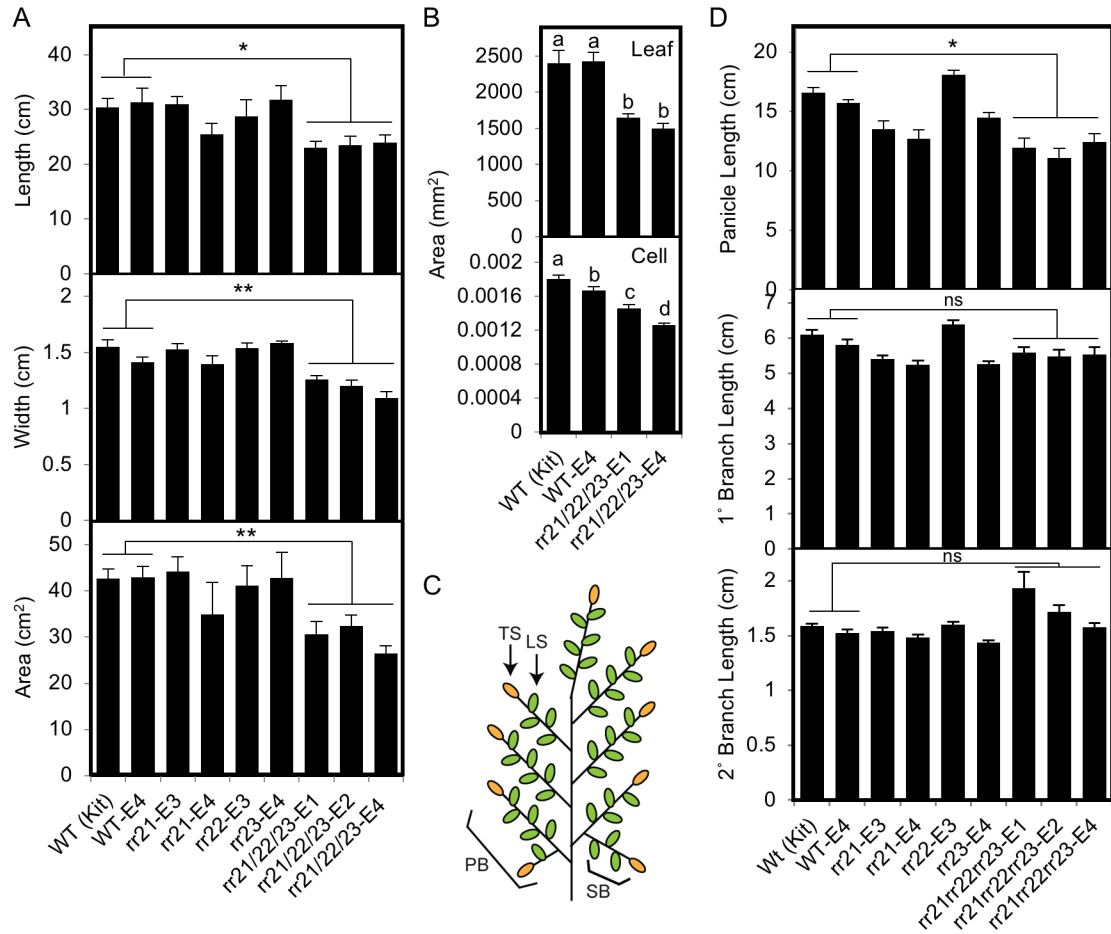
**Fig. S3.** Leaf and panicle phenotypes of type-B *RR* mutants. **A,** Flag leaf length, width, and area for wild type, single, and triple *RR* mutant lines. **B,** Flag leaf area and cell area for experiment shown in Fig. 1C. Different letters indicate significant difference, P < 0.05. **C,** Illustration showing panicle characteristics, including primary branch (PB), secondary branch (SB), lateral spikelet (LS), and terminal spikelet (TS). **D,** Panicle length, primary branch length, and secondary branch length for the experiment shown in Fig. 1D. For data comparison of *rr21/22/23* lines to wild type, ANOVA analysis was performed with post hoc Holm multiple comparison calculation (*P < 0.05, **P < 0.01; ns = not significant at $P_{0.05}$; error bars = SE).
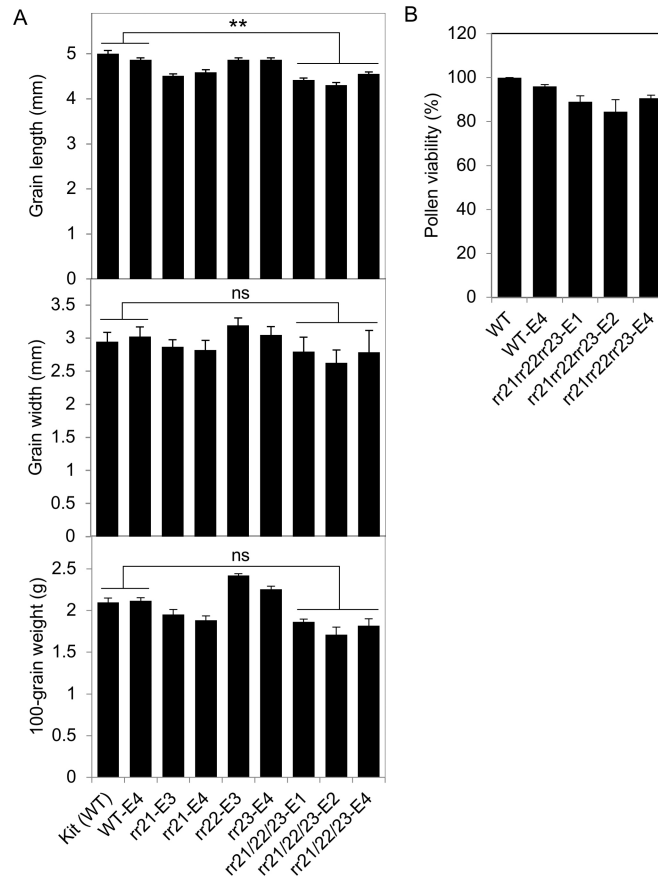
**Fig. S4.** Fertility and trichome related phenotypes of *rr21/22/23*. **A,** Grain length, width, and 100-grain weight. For data comparison of *rr21/22/23* lines to wild type, ANOVA analysis was performed with post hoc Holm multiple comparison calculation (**P < 0.01; ns = not significant at $P_{0.05}$; error bars = SE). **B,** Pollen viability of *rr21/22/23* lines compared to the wild type.
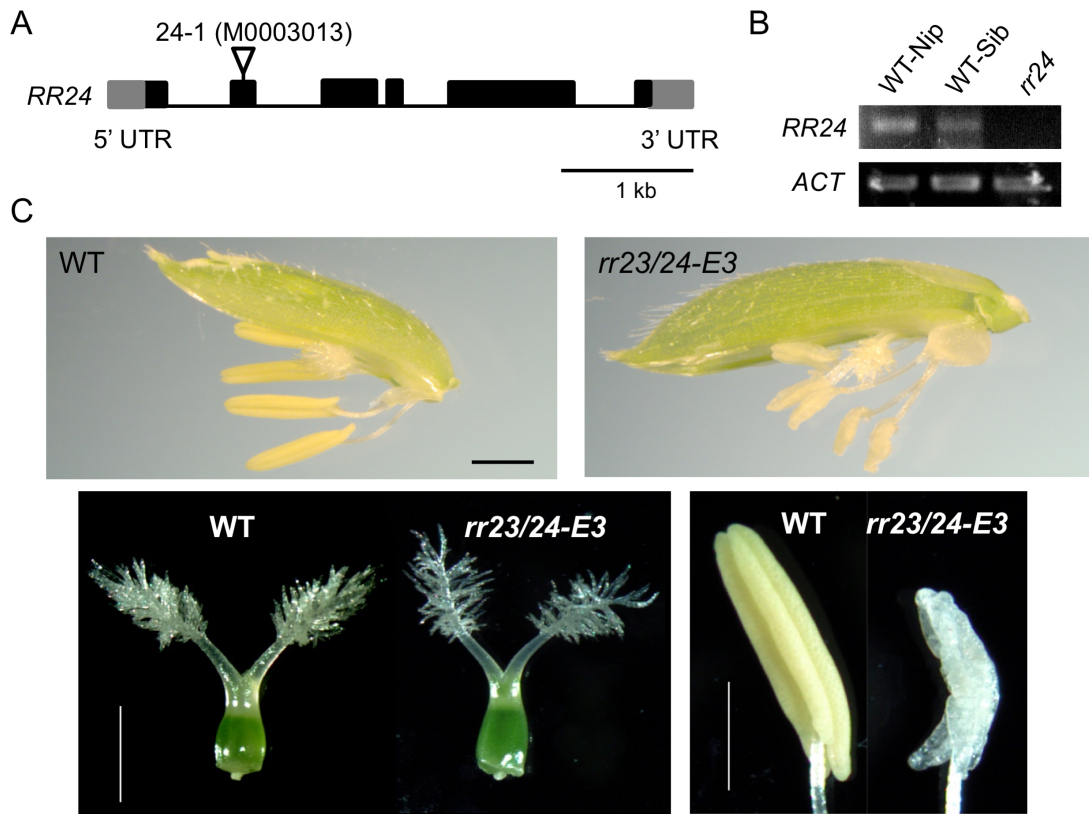
**Fig. S5.** Characterization of *rr24* mutants. **A,** Diagram of T-DNA insertion site of *rr24-1*. **B,** RT-PCR demonstrating lack of full-length transcript for the *rr24* T-DNA insertion mutant. Actin (*ACT*) is the control. **C,** The CRISPR/Cas9-generated *rr23/24* mutant exhibits defective anther development. Scale bars = 1 mm.
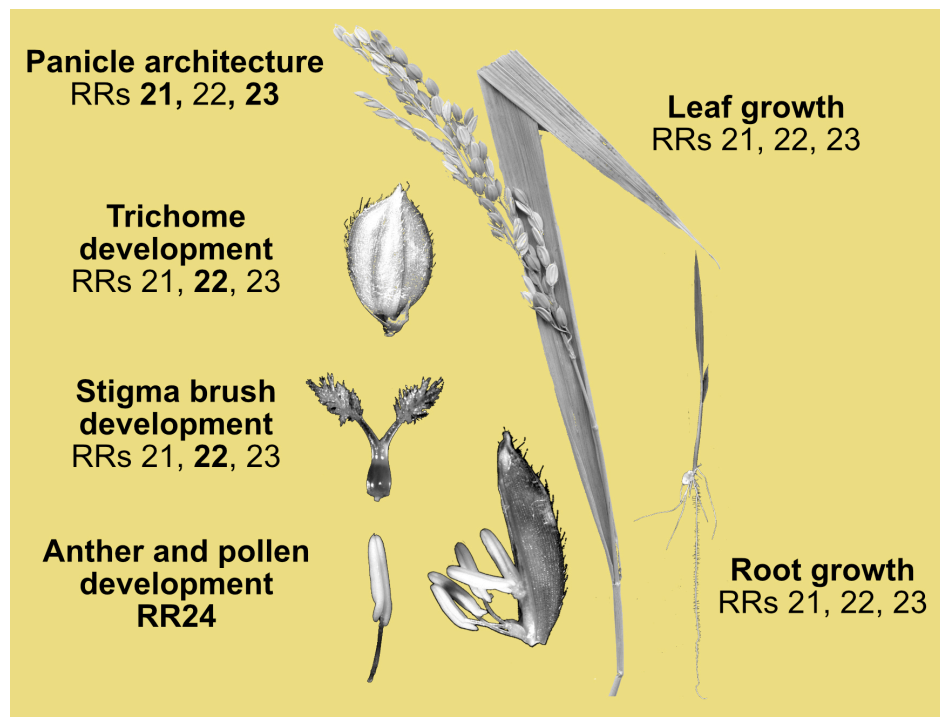
**Fig. S6.** Developmental roles of type-B RRs in rice. Type-B RRs implicated in each role by genetic analysis are indicated, with major contributors in bold.

**Table S1. CRISPR/Cas9 induced mutations**

| Gene | Genotype | Target Sequence (5' - 3')[1] |
|---|---|---|
| *RR21* | WT | CGTGGGGATGAAGGTGCTGG |
| | 1-bp insertion (G) Event 1 | CGTGG**G**GGGATGAAGGTGCTGG |
| | 1-bp insertion (T) Event 2 | CGTG**T**GGGATGAAGGTGCTG |
| | 1-bp insertion (C) Event 3 | CGTG**C**GGGATGAAGGTGCTG |
| | 13-bp deletion (GGGATGAAGGTGC)/6-bp insertion (CCACCA) Event 4 | CGTGG**CCACCA***AAGGTGTGG* |
| *RR22* | WT | ATCAATTCCCCGTCGGCATG |
| | 1-bp insertion (A) Event 2 | ATCAATTCCC**A**CGTCGGCAT |
| | 1-bp insertion (C) Event 4 | ATCAATTCCC**C**CGTCGGCAT |
| | 1-bp insertion (T) Events 1 and 3 | ATCAATTCCC**T**CGTCGGCAT |
| *RR23* | WT | AGGAGGGACCAGTTCCCCGT |
| | 1-bp insertion (A) Events 1, 2, and 4 | AGGAGGGACCAGTTCCC**A**CG |
| | 1-bp deletion (C) Events 3 and 4 | AGGAGGGACCAGTTCCC*C*GT |
| *RR24* | WT | ACCAGTTCCCGGTCGGCATGCGGGTGCT |
| | 7-bp deletion (CATGCGG) Event 3 | ACCAGTTCCCGGTCGG*CATGCGG*GTGCT |

[1]Insertions in bold (red); deletions in bold italics (blue)

**Table S2. CRISPR/Cas9 lines used in this study**

| Genotype-Event (Generation isolated) | rr21 | rr22 | rr23 | rr24 |
|---|---|---|---|---|
| WT-E4 | (+/+) | (+/+) | (+/+) | (+/+) |
| *rr21-E3* (T4) | (-/-) 1-bp ins (C) | (+/+) | (+/+) | (+/+) |
| *rr21-E4* (T4) | (-/-) 13-bp del (GCACCTTCATCCC) / 6-bp insertion (CCACCA) | (+/+) | (+/+) | (+/+) |
| *rr22-E3* (T3) | WT | (-/-) 1-bp ins (T) | WT | (+/+) |
| *rr23-E4* (T2) | WT | (+/+) | (-/-) 1-bp del (C) | (+/+) |
| *rr21/22/23-E1* (T2) | (-/-) 1-bp del (G) | (-/-) 1-bp ins (T) | (-/-) 1-bp ins (A) | (+/+) |
| *rr21/22/23-E2* (T3) | (-/-) 1-bp ins (T ) | (-/-) 1-bp ins (A) | (-/-) 1-bp ins (A) | (+/+) |
| *rr21/22/23-E4* (T4) | (-/-) 13-bp del (GCACCTTCATCCC) / 6-bp insertion (CCACCA) | (-/-) 1-bp ins (C) | (-/-) 1-bp ins (A) | (+/+) |
| *rr23/24-E3* (T2) | (+/+) | (+/+) | (-/-) 1-bp del (C) | (+/-) 7-bp del (CATGCGG) |

**Table S3. Primers used in this study**

| Gene | Forward primer (5' to 3') | Reverse primer (5' to 3') |
|---|---|---|
| Genotyping primers | | |
| *RR21* | TTTTCGGTTTCGTGGGCG | CGACTCCTCCCCAACCC |
| *RR22* | ATGCTTCTGGGTGCTTTGAG | GCCAAGTATGCTAGTATCAGTGA |
| *RR23* | TGAATCCCAATCTTCCCCTG | CAGCTTCTTTCTTTCCATTTTGC |
| *RR24* | TGTTTCTTGGGTTGCTTGGAG | GGTCAGCAGAAGATAATCCTTACA |
| *HygR* | GCCGCGCTCCCGATTCCGGA | GCTCGAAGTAGCGCGTCTGCT |
| *RR24 (T-DNA)* | TTGCACACATGGTGGTTGTGT | TCCATCTCGAGGCCGACAAGC |
| *pTAG4-RB* | ACTCATGGCGATCTCTTACC | |
| qPCR primers | | |
| *RR6* | CATCACCGACTACTGGATGC | GGGATCTCCTTGAGCTGAGA |
| *RR9/10* | TCATGAGGACAGCCCAATTTCTA | TGCAGTAGTCTGTGATGATCAGGTT |
| *CKX5* | CCCCATGAACAGGCACAAGT | GAGGATCTCCCGGTTCTGCC |
| *GL3a* | CCAGCAGCAGCGAAAATACA | GAAGCCGTCCTTCCAAGTCA |
| *HOX2* | TCGCCATGACAAACTTGGGA | TCCCCTCCTCTTGAGTGATT |
| *NPR5/BOP1* | TTCGGGAAGATGAACGACGG | GAAGCCATGTGGGGAGAACA |
| *EXPA6* | AAATCCCTACGCAGTGCCAG | TTGGGGTAGTTTGGTGCGTT |
| *WDA1* | AACACTTACCGCTGTGGAGG | TAGGCAACGAGCTCAGCAAA |
| *GH3.1* | CTCCATACCGCTGCCTACAT | TTGTGCTCCCTGGATTTCGG |
| *SAUR54* | CGCTTCGAGGTTCCACTGAT | TCAGGAGCGCCTTCTCAATC |
| *WOX3B* | CACGCTAATTCCCTTCTCTC | TAGTAGTAGCTGGTGGTGTAA |
| *HL6* | ACCTGTGGGACAATAGCTGC | AGTGATCAACAATGTAACGTCCA |
| *UBQ5* | ACCACTTCGACCGCCACTACT | ACGCCTAAGCCTGCTGGTT |

## References

**Dereeper, A., Guignon, V., Blanc, G., Audic, S., Buffet, S., Chevenet, F., Dufayard, J. F., Guindon, S., Lefort, V., Lescot, M., et al.** (2008). Phylogeny.fr: robust phylogenetic analysis for the non-specialist. *Nucleic Acids Res* **36**, W465-469.

**Schaller, G. E., Kieber, J. J. and Shiu, S.-H.** (2008). Two-component signaling elements and histidyl-aspartyl phosphorelays. *The Arabidopsis Book (C. Somerville, E. Meyerowitz, editors)* **6**, e0112.

**Tsai, Y. C., Weir, N. R., Hill, K., Zhang, W., Kim, H. J., Shiu, S. H., Schaller, G. E. and Kieber, J. J.** (2012). Characterization of genes involved in cytokinin signaling and metabolism from rice. *Plant Physiol* **158**, 1666-1684.

**Yamburenko, M. V., Kieber, J. J. and Schaller, G. E.** (2017). Dynamic patterns of expression for genes regulating cytokinin metabolism and signaling during rice inflorescence development. *PLoS One* **12**, e0176060.